Title:

Cardiac competence of the paraxial head mesoderm fades concomitant with a shift towards the head skeletal muscle programme

Running title:

Cellular competence of the paraxial head mesoderm

Afnan Alzamrooni[1], Petra Mendes Vieira[1], Nicoletta Murciano[1,2,3], Matthew Wolton[1] and Susanne Dietrich[1]*

[1] Institute of Biological and Biomedical Sciences
School of Pharmacy and Biomedical Sciences
University of Portsmouth
Portsmouth, UK

[2] Nanion Technologies GmbH, Ganghoferstr. 70A, DE - 80339 München, Germany.

[3] Saarland University, Theoretical Medicine and Biosciences, Kirrbergerstr. 100, DE - 66424 Homburg, Germany

***Corresponding author:**

Susanne Dietrich, Institute of Biological and Biomedical Sciences, School of Pharmacy and Biomedical Sciences, University of Portsmouth, St. Michael's Building, White Swan Road, Portsmouth, PO1 2DT, UK
T: +44 (0)2392 84 2959
F: +44 (0)2392 84 3565
E: susanne.dietrich@port.ac.uk
W: http://www.port.ac.uk/institute-of-biological-and-biomedical-sciences/epigenetics-and-developmental-biology/susanne-dietrich/Portsmouth, UK
ORCID iD: https://orcid.org/0000-0001-8688-8992

Summary statement:

The head mesoderm has generic cardiac competence until early head fold stages. Thereafter, cardiac competence fades in the paraxial region, and Bmp promotes head skeletal muscle programmes instead of cardiac programmes.

Abstract

The vertebrate head mesoderm provides the heart, the great vessels, some smooth and most head skeletal muscle, in addition to parts of the skull. It has been speculated that the ability to generate cardiac and smooth muscle is the evolutionary ground-state of the tissue. However, whether this is true, how long this generic cardiac competence may last, and what happens as cardiac competence fades, is not clear.

Bone morphogenetic proteins (Bmps) are known to promote cardiogenesis. Using a wide palette of marker genes in the chicken embryo, we show that the paraxial head mesoderm that normally does not engage in cardiogenesis has the ability to respond to Bmp for a long time. However, Bmp signals are interpreted differently at different time points. Up to early head fold stages, the paraxial head mesoderm is able to read Bmps as signal to engage in the cardiac programme; the ability to upregulate smooth muscle markers is retained slightly longer. Notably, as cardiac competence fades, Bmp promotes the head skeletal muscle programme instead. The switch from cardiac to skeletal muscle competence is Wnt-independent as Wnt caudalises the head mesoderm and suppresses both the cardiac and the head skeletal muscle programmes. This finding points at an intrinsic control mechanism.

Our study for the first time suggests a specific transition state in the embryo when cardiac competence is replaced by skeletal muscle competence. It sets the stage to unravel the cardiac-skeletal muscle antagonism that is known to partially collapse in heart failure.

Keywords

Vertebrate embryos, head mesoderm, heart, head skeletal muscle, developmental competence, Bmp, Wnt.

1. Introduction

The vertebrate head mesoderm is the first embryonic mesoderm type to emerge during gastrulation (Camp et al., 2012; Garcia-Martinez and Schoenwolf, 1993). It delivers the heart (reviewed in (Meilhac and Buckingham, 2018; Sendra et al., 2021; Spater et al., 2014)), the great vessels (Paffett-Lugassy et al., 2013; Wang et al., 2017), the smooth muscle collar of the cardiac outflow (Wang et al., 2017), genuine craniofacial and oesophageal skeletal muscles (reviewed in (Schubert et al., 2018)) and parts of the skull ((Jandzik et al., 2015); reviewed in (Kuratani, 2005)), with cardiac cells originating from the lateral, and skeletal muscle and also bone/cartilage mainly from the paraxial region of the tissue (reviewed in (Evans and Noden, 2006)). The primitive heart, blood and vascular system are the first fully functional organs in the embryo, and defects in their development are incompatible with life. In recent years, the head mesoderm has received quite some attention since a subpopulation of cardiogenic cells, often referred to as secondary heart field (SHF) cells and located in the pharyngeal arches at the junction to the primitive heart, seem to be multipotent cardiac-skeletal muscle-vascular endothelial precursor or stem cells (reviewed in (Sendra et al., 2021)). When these cells are recruited into the primitive heart, they deliver the mature in- and outflow tract, in mammals and birds also encompassing the right ventricle. This process is essential as compromised SHF formation causes cardiac birth defects (reviewed in (Houyel and Meilhac, 2021; Morton et al., 2022)). Notably, SHF cells integrate perfectly into the developing heart and beat according to the rhythm set by the pre-existing cells. This is in stark contrast to cells transplanted into an adult heart to replace cells lost after a heart attack: here, cells struggle to integrate, and their autonomous beating may cause potentially fatal arrhythmias (Cui et al., 2018; Scuderi and Butcher, 2017; Spater et al., 2014). In a similar vein, the embryo is able to allocate head mesodermal cells to various conflicting developmental programmes. Yet in a failing heart, cells partially lose their cardiomyocyte identity and erroneously express skeletal muscle genes (reviewed in (Oh et al., 2019)). Thus, sustained efforts aim to understand the properties and developmental programmes of cells in the embryonic head mesoderm in order to apply this understanding to diagnosis and treatment of disease.

Transcriptome analyses and grafting experiments showed that the head mesoderm is distinct from the mesoderm in the trunk that does not normally deliver cardiomyocytes and that forms skeletal muscle using distinct programmes (reviewed in (Schubert et al., 2018)). Comparative analyses between vertebrates and invertebrate chordates indicated that this head-trunk distinction is basic to chordates. Originally, chordates lacked mesoderm-derived cartilage and bones; skeletal (voluntary)

muscle served the purpose of locomotion and formed from the trunk paraxial mesoderm (somites). Contractile tissue in the head existed in form of pharyngeal smooth muscle and cardiac muscle placed upstream of the vessels supplying the pharyngeal basket/pharyngeal arches (reviewed in (Poelmann and Gittenberger-de Groot, 2019; Simões-Costa et al., 2005). Recent analyses of the core regulatory complexes controlling muscle formation suggested that the striated organisation of cardiac muscle originated from a recruitment of downstream skeletal muscle effector genes into pre-existing smooth muscle programme (Brunet et al., 2016). Thus, we hypothesised that the evolutionary default programme of the head mesoderm was to deliver cardiac and smooth muscle. However, with the acquisition of an active, predatory lifestyle, vertebrates seem to have recruited further aspects of the skeletal muscle programme into the head mesoderm, including the MyoD-type core regulators of the voluntary/skeletal muscle programme. If this idea were to be correct, we would expect to see a switch from cardiac to skeletal muscle competence in the paraxial head mesoderm (PHM) which does not normally partake in cardiogenesis. The aim of this study was to investigate this idea.

Cells fated to contribute to the heart are specified, but not yet determined, as cardiogenic cells when they leave the primitive streak ((Lopez-Sanchez et al., 2009; Wang et al., 2013); reviewed in (Sendra et al., 2021)). Migration to their target area lateral to the developing neural plate is controlled by bone morphogenetic proteins (Bmp; ((Song et al., 2014)). Moreover, Bmps are essential for cardiogenic cells to realise their potential and differentiate into cardiomyocytes (reviewed in (Cui et al., 2018; Spater et al., 2014; van Wijk et al., 2007)). Bmps drive cardiogenesis indirectly by suppressing the proliferation-promoting function of fibroblast growth factors (Hutson et al., 2010; Tirosh-Finkel et al., 2010). They also control cardiogenesis directly, with Smad1/5/8-Smad4 complexes transactivating genes encoding key cardiac transcription factors such as Isl1, Nkx2.5, Gata4 and Tbx2 (Brown et al., 2004; Hami et al., 2011; Liberatore et al., 2002; Lien et al., 2002; Shirai et al., 2009; Si et al., 2014). Before and during the formation of the primitive heart, the Bmp ohnologs Bmp2 and 4 are expressed in the lateral and extraembryonic mesoderm, its overlying ectoderm and underlying pharyngeal endoderm and the neural folds. Bmp2 continues to be expressed in the cardiac inflow tract, Bmp4 in the SHF adjacent to the heart. The heart expresses Bmp7 throughout, the ventricle expresses Bmp10. Thus, the lateral head mesoderm is under the influence of Bmp all the time. In contrast, the paraxial head mesoderm is exposed to the Bmp inhibitors Noggin and Chordin delivered by Hensen's node and the notochord in the midline of the embryo ((Bothe et al., 2011), http://geisha.arizona.edu/geisha/; for Bmp phylogeny see (Hinck et al., 2016; Huminiecki et al., 2009)). Moreover, various studies showed that exposure to Bmp can trigger the expression of cardiac markers in the PHM (Andree et al., 1998; Bothe et al., 2011; Schlange et al.,

2000; Schultheiss et al., 1997; Tirosh-Finkel et al., 2006; von Scheven et al., 2006a; Yamada et al., 2000). However, whether the PHM has full cardiac competence (i.e. can complete differentiation), and how long this competence may last is currently unclear since different experimental approaches have led to different results (compilation of these approaches in Supplementary Figure SF1). Interestingly, Bmp7 is expressed in the early prechordal plate and later, in the pharyngeal arches (von Scheven et al., 2006a). It thus is in the position to signal to the developing branchiomeric skeletal muscles. Moreover, Bmp signalling has been shown to activate the expression of *Msc* (Bothe et al., 2011), a gene in the head involved in the activation of the first MyoD family member to be expressed, namely *Myf5* ((Moncaut et al., 2012), reviewed in (Schubert et al., 2018)). We therefore reasoned that a strict exposure regime to Bmp would reveal the initial and any shift in cellular competence of the PHM. Our study shows that this indeed was the case: differing, stage-dependent responses to Bmp indicate a shift from cardiac to skeletal muscle competence in the PHM.

Beta Catenin-mediated Wnt signalling plays multiple roles during cardiac development (reviewed in (Gessert and Kühl, 2010). Wnt signalling is required for gastrulation, and hence without Wnt, cardiogenic cells cannot form (Kraus et al., 2016). Wnt signals deflect the early gastrulating cells from the primitive streak and hence contribute to the congregation of cardiogenic cells in the lateral head mesoderm (Song et al., 2014; Yue et al., 2008). However, prolonged Wnt signals also contribute to the caudalisation of the gastrulating mesoderm, thus establishing the trunk programmes and suppressing cardiogenesis (Marvin et al., 2001). To escape this inhibition, cardiac precursors are bestowed with the expression of Wnt inhibitors such as Szl (also called Sfrp2- or Sfrp5 related; (Wittler et al., 2008), reviewed in (Wu et al., 2020)). Previous studies proposed that an increase in paraxial beta Catenin-dependent Wnt signalling may suppress the ability of the PHM to engage in cardiogenesis (Tzahor and Lassar, 2001). We therefore also tested whether Wnt signalling may promote the switch from cardiac to skeletal muscle competence in the PHM. However, this was not the case: Wnt suppressed the onset of the head skeletal muscle programme, suggesting that the switch in developmental competence is intrinsic to the PHM.

2. Material and Methods

2.1. Chicken embryo culture, staging and harvesting

Wildtype fertilised chicken eggs were obtained from Henry Stewart & Co. (Lincolnshire, UK), eggs from GFP-expressing chicken were obtained from the National Avian Research Facility

(https://www.ed.ac.uk/roslin/national-avian-research-facility). Eggs were incubated at 38.5°C in a humidified incubator (LMS) and staged according to (Hamburger and Hamilton, 1951). For bead and GFP-tissue implantation experiments at HH5-10, embryos were cultured as 'EC-cultures' on filter rings as described by Chapman and Bothe (Bothe et al., 2011; Chapman et al., 2001). Experiments at HH13/14 were performed in ovo. All embryos were harvested in 4% PFA.

2.2. Recombinant proteins and bead preparation

Recombinant Bmp proteins from R&D Systems/Biotechne (Bmp2: 355-BM-10, Bmp4: 314-BP-10, Bmp7: 354-BP-10, Bmp10: 2926-BP-025) were reconstituted in 4mM HCl supplemented with 0.1% bovine serum albumin at a concentration of 1mg/ml or 0.5mg/ml. Affi-Gel blue agarose beads (BioRad) and heparin-coated acrylic beads (Sigma) suspended in sterile water were added to obtain 0.19µM, 1.28µM, 6.41µM or 19.23µM dilutions. Wnt3a protein from R&D Systems/Biotechne (5036-WN-010) was reconstituted in PBS with 0.1% bovine serum albumin at 0.4mg/ml, beads in diluted in sterile water were added to obtain 5.35-10.7µM dilutions. No difference in phenotypes for the different Wnt3a concentrations were observed with the most sensitive marker *Cyp26C1*, and the experiments were then carried out with 8.56µM Wnt3a and the data combined. The beads were soaked in these solutions for an hour on ice, then washed in saline before grafting. Control beads were soaked in 0.1% BSA in saline.

2.3. Bead implantation

Beads were grafted into the paraxial head mesoderm (PHM) of HH5/6, HH7/8 and HH9/10 embryos on EC culture plates and HH13/14 embryos in ovo, using flame-sharpened tungsten needles as described in (Bothe et al., 2011; von Scheven et al., 2006a). For HH5/6 and HH7/8, embryos were accessed from the ventral side; HH9/10 embryos were accessed from the dorsal side. Unless stated otherwise, beads were implanted into the central PHM as shown in Supplementary Figure SF1. Beads for the lateral/cardiogenic head mesoderm were implanted into EC-culture embryos from the ventral side. The embryos were incubated for 6 hours, during which time they progressed to the next stage of development. For the time course experiment, embryos were incubated for 2, 4 and 6 hours. To allow for the response of indirect targets further downstream in regulatory cascades and for cardiac differentiation, embryos were also incubated overnight.

2.4. GFP-tissue implantation

GFP expressing donor embryos were mounted on filter rings, washed in saline and pinned down on Sylgard-bottomed Petri dishes as described in (Alvares et al., 2008). To extract the HH5/6 and 7/8 PHM and HH5/6 cardiac mesoderm, donors were ventral side up. Using a glass capillary mounted on an aspirator, a small drop of 1mg/ml Dispase (Sigma) in DMEM was delivered to the to-be-excised

region, then the endoderm was peeled off using flame-sharpened, angled 0.1mm tungsten needles. Using these needles, the PHM was cut free from the region inside the neural plate territory, the lateral/cardiac mesoderm was excised from the territory lateral to the neural plate. The tissue was transferred into saline with a further glass capillary and aspirator to wash off excess Dispase, cut into smaller fragments, and transferred to the hosts set up as EC-cultures. A small incision was made at the desired location. This released tissue tension, delivering an opening to fit in the graft.

To recover the HH9/10 PHM, the donor was pinned down dorsal side up, and Dispase was applied. Using the tungsten needles, an incision was made into the surface ectoderm parallel to the neural tube, and the ectoderm plus adhering neural crest cells were peeled away. The PHM was eased away from the neural tube medially and from the surface ectoderm and lateral mesoderm laterally, cut free rostrally and, with a distance to the 1st somite caudally, and lifted out of the slit. It was washed, cut and transferred as described before.

To recover the HH13/14 PHM, the embryo was pinned down, with pins holding the head in place. Dispase was delivered to the region dorsal to the pharyngeal arches, and the surface ectoderm plus adhering neural crest cells was removed. Using the tungsten needles, a piece of mesenchyme was retrieved, washed, and implanted as before.

To excise the HH13/14 segmental plate, the donor was pinned down ventral side up, the endoderm was removed with the help of Dispase, the segmental plate was freed from the neural tube and lateral mesoderm, cut at the dorsal and ventral end, and again, washed, cut into smaller fragments and implanted.

2.5. Generation of templates and probes for in situ hybridisation

Probes for in situ hybridisation and wildtype gene expression patterns are summarised in Supplementary Spreadsheet SS1. Templates for probe synthesis were generated using restriction endonucleases or by PCR with plasmid-based primers; antisense probes were made using the appropriate T3/T7/sp6 RNA polymerases and the DIG labelling mix (Roche/Sigma), following the manufacturer's instructions.

2.6. In situ hybridisation

In situ hybridisation was performed following the procedure of (Bothe et al., 2011). Embryos were permeabilised first in methanol overnight, then with a detergent mix (3 x 6 minutes for young embryos, 3 x 10 minutes for embryos at HH13/14). They were re-fixed in 4% PFA for 20 minutes and equilibrated in pre-hybridisation mix for 1 hour. Hybridisation was performed overnight at 70°C; probes were detected using the alkaline phosphatase-coupled anti-DIG antibody (1:2000, Roche/Sigma) and NBT/BCIP (Roche/Sigma). The hybridisation- and antibody-step were performed

using a CEM InsituPro robot. After staining, embryos were fixed in 4% PFA overnight and stored in 80% glycerol.

2.7. Immunofluorescence

Immunofluorescence followed the procedure described in (Berti et al., 2015; Meireles Nogueira et al., 2015), using the mouse MF20 (1:500, DSHB) and the rabbit anti-GFP (1:1000, Life technology) primary antibodies, and the anti-mouse IgG+IgM (H+L) – Alexa fluor 594 and the anti-rabbit (H+L) – Alexa fluor 488 secondary antibodies (1:300, Jackson Immuno).

2.8. Photomicroscopy

Images were captured on a Zeiss Axioskop with DIC and fluorescence optics, using a Zeiss AxioCam digital camera with ZEN light software. Confocal images were captured on a Zeiss LSM 710 microscope. Images were processed using Adobe Photoshop 6.0. To photograph the heads of embryos treated at HH13/14, embryos were bisected midsagitally, using flame-sharpened tungsten needles.

3. Results

3.1. Responsiveness of the PHM to Bmp and Wnt/beta Catenin signalling

Aim of the study was to explore the cardiac competence of the paraxial head mesoderm (PHM) as revealed by its stage-dependent responses to Bmp signalling. We focused on the chicken embryo because of its large size, clear anatomy and ease of access, and because it is an established model for vertebrate, including human, head mesoderm and heart development (reviewed in (Wittig and Münsterberg, 2020)). Since we previously had found dynamic changes in gene expression pattern and mesodermal behaviour in the PHM between developmental stages HH5/6 and HH9/10 (Bothe and Dietrich, 2006; Bothe et al., 2011), and because it has been proposed that Wnt levels triggering the beta-Catenin pathway may rise in this time period (Tzahor and Lassar, 2001), we also tested whether Wnt signalling was responsible for a change in the developmental competence of the PHM. Studies exposing the PHM to Bmp and Wnt signalling have been done before. However, these studies used different ligands, different delivery methods, different treatment durations and different marker genes ((Andree et al., 1998; Bothe et al., 2011; Marvin et al., 2001; Schlange et al., 2000; Schultheiss et al., 1997; Song et al., 2014; Tirosh-Finkel et al., 2006; Tzahor and Lassar, 2001; von Scheven et al., 2006a; Yamada et al., 2000; Yue et al., 2008) summarised in Supplementary

Figure SF1)). We therefore as a first step in our study established a robust and also systematic and strict experimental approach.

3.1.1. Preparatory experiments to establish a strict experimental approach

When signalling molecules are delivered by biological carriers such as expression constructs or engineered cells, there is little control over the concentrations of the ligands. We therefore used recombinant proteins loaded onto carrier beads and established in early, Bmp- and Wnt-sensitive embryos that micromolar ranges of ligand triggered responses within 6 hours irrespective of the bead type used (Supplementary Figure SF2.A-D). Given that different Bmp molecules may elicit different responses (Klumpe et al., 2022), we established that the Bmps associated with heart and lateral mesoderm development, namely the ohnologs Bmp2 and Bmp4 and the more distantly related paralogs Bmp7 and 10 (Hinck et al., 2016; Huminiecki et al., 2009), will trigger the same responses (Supplementary Figure SF2.E-N). A time-course experiment showed that known Bmp- and Wnt/beta Catenin- sensitive genes are transcriptionally up- or downregulated within 2-4 hours, thus a 6 hours treatment regime will allow to detect robust responses of direct and first-wave indirect target genes (Supplementary Figure SF3). Bmp has been shown to not only influence head mesodermal gene expression but also cardiac cell migration (Song et al., 2014). We therefore tested whether, within 6 hours of treatment, cells would be attracted or deflected by the Bmp-bead. This however was not the case (Supplementary Figure SF4). All n-number for the preparatory and all the following bead experiments are provided in Supplementary spreadsheet SS1).

3.1.2. Test for the PHM's responsiveness to Bmp and Wnt

Having established that Bmp and Wnt ligands delivered on heparin-coated acrylic beads robustly affect gene expression within 6 hours, we now tested whether the PHM at stages HH5/6, HH7/8, HH9/10 and HH13/14 is responsive to Bmp and Wnt. These stages were selected because of earlier observations on stage-specific expression patterns and responses to signalling molecules: at HH5/6, genes driving cardiac development and the first PHM genes are expressed, at HH7/8 the next set of PHM genes becomes activated, at HH9/10, specifically *Msc* (=*MyoR*), a gene controlling the activation of *Myf5* in head skeletal muscle precursors is activated, and at HH13/14 head skeletal muscle differentiation commences ((Bothe and Dietrich, 2006; Bothe et al., 2011; Meireles Nogueira et al., 2015; Moncaut et al., 2012); summarised in Supplementary Figure SF1)). For our first test, we focused on *Msx2*, a direct Bmp target (Sirard et al., 2000), and *Lef1*, a direct Wnt/beta Catenin target gene (Li et al., 2006). *Msx2* is initially expressed in the early lateral mesoderm and the neural folds/ dorsal neural tube; later expression occurs at many sites including the distal aspect of the pharyngeal arches (http://geisha.arizona.edu/geisha/), where the gene contributes to the survival of

SHF cells (Chen et al., 2007). We found that Bmp2 strongly activated *Msx2* transcription in the head mesoderm and the neural tube at all stages (Fig1.A-D, green arrowheads). Upregulation also occurred in the HH13/14 neural crest cells and the somites (Fig.1Dii,iii, green arrowheads). *Lef1* is initially expressed in the developing somites and in the caudal aspect of the PHM; later expression domains include the pharyngeal arches, cranial ganglia and the optic cup (http://geisha.arizona.edu/geisha/). We found that Wnt3a effects on *Lef1* were more subtle. At HH5/6 through to HH9/10, Wnt3a rostrally expanded the expression domain of *Lef1* in the caudal PHM (Fig.1E-G, green arrowheads). Occasionally, *Lef1* was also slightly upregulated around a Wnt3a-bead located in the rostral PHM (not shown). At HH13/14, Wnt3a upregulated *Lef1* expression in the pharyngeal arches, the neural tube and in the trunk ectoderm (Fig.1H, green arrowheads). Taken together, this suggests that the PHM is highly sensitive to Bmp. It has more limited sensitivity to Wnt or is better protected against Wnt.

3.2. Response of heart-promoting transcription factors to Bmp-treatment at different stages of development

As the PHM is sensitive to Bmp at all the stages investigated, we now were in the position to ask: Will Bmp induce the cardiac programme at all stages? Cardiogenesis is initiated by a combination of transcription factors including Isl1, Nkx2.5, Tbx2, Tbx5, Hand2 and Gata4. Mesodermal cells expressing the pioneer factor Isl1 are thought to still have non-cardiogenic options, however the expression of Nkx2.5 drives cells towards a cardiomyocyte fate (Gao et al., 2019; Jia et al., 2018). Importantly, Nkx2.5 is not sufficient for cardiomyocyte differentiation, and it is the combinatorial expression of cardiogenic transcription factors that allows beating cardiomyocytes to form, both in vivo and in vitro (Ieda et al., 2010; Luna-Zurita et al., 2016; Zhou et al., 2012). We therefore included all these markers in our analysis. It has to be considered, however, that their expression patterns are overlapping but not identical: in wildtype embryos, all are expressed in the splanchnic lateral mesoderm that delivers the primitive heart and thus they are associated with cardiogenic precursor cells. *Isl1, Nkx2.5, Tbx2* and *Hand2* expression is maintained in the distal pharyngeal arches that contain the secondary heart field (SHF); *Gata4* and *Tbx5* expression are maintained in the caudal SHF; *Tbx5* expression eventually becomes confined to the inflow tract and atria; *Isl1* is switched off in differentiating cells. Notably, *Isl1*, *Nkx2.5* and *Tbx2* are also expressed in the pharyngeal endoderm; *Isl1* is further expressed in the dorsal neural tube and cranial ganglia; *Hand2, Gata4, Tbx2* and *Tbx5* are more widely expressed, including the lateral and extraembryonic mesoderm of the trunk (http://geisha.arizona.edu/geisha/).

Implantation of Bmp2-beads into the PHM triggered expression of all the cardiac marker genes at HH5/6 (Fig.2A,E,I,M,Q,U; green arrowheads). Upregulation was strong for *Isl1, Nkx2.5, Hand2* and *Gata4*, robust for *Tbx2* and more limited for *Tbx5*, likely because *Tbx5* is an indirect target (see also (Yamada et al., 2000)). Notably, at HH7/8, Bmp2 failed to activate *Tbx5* in the PHM (Fig.2V, blue arrowhead), and from HH9/10 onwards, Bmp2 failed to activate *Gata4* (Fig.2S, blue arrowhead). At HH13/14, Bmp-beads dorsally expanded the expression domains of *Isl1* and *Hand2* which are normally confined to the distal/ventral pharyngeal arches that contain the SHF (Fig.2 Dii, Pii, green arrow). However, ectopic expression around the bead was not observed. Moreover, expression of *Nkx2.5*, *Tbx2*, *Gata4*, *Tbx5* was unchanged (Fig.2 Hii, Lii, Tii, Xii, blue arrowheads). When Bmp-beads were implanted into the trunk paraxial mesoderm, i.e. the somites, expression of *Tbx2*, *Hand2*, and *Gata4* was upregulated (Fig.2Liii, Piii, Tiii, green arrowheads); the other markers did not respond. The activation of these more general lateral mesoderm markers suggests that Bmp can 'lateralise' the paraxial mesoderm for some time, both in the head and in the trunk. However, the ability of Bmp to activate the full cardiac marker set fades away after stage HH5/6.

3.3. Cardiac differentiation of the PHM

The activation of the complete set of cardiac precursor markers at stage HH5/6 suggested that at this stage, the PHM has full cardiac competence. However, using the same 6-hour treatment regime, Bmp did not activate *Myocd*, *Mef2c* and cardiac effector genes, even when higher concentrations were used (Supplementary Figure SF5). Yet in the embryo it takes some 14 hours from stage HH5/6 to HH10 when the first cardiomyocytes are terminally differentiated and the heart begins to beat (reviewed in (Wittig and Münsterberg, 2020)). We thus allowed the beaded embryos to develop for 16-18 hours overnight. Moreover, we trebled the Bmp concentrations to compensate for diffusion away from the bead. Terminal differentiation was revealed by immunofluorescence with the MF20 antibody which recognises sarcomeric myosins (Fig.3, red staining). Notably, at elevated concentrations, Bmp2 triggered ectopic sarcomeric myosin expression in the PHM, but only when the bead was inserted at HH5/6 (Fig.3L, green arrowhead).

The implantation of Bmp-loaded beads only partially mimics the complement of factors cardiogenic cell are normally exposed to. Moreover, the Bmp concentrations used here may be artificially high. We therefore tested whether the PHM can complete differentiation in a natural cardiogenic environment. To achieve this, the PHM was excised from GFP expressing embryos and transplanted into the cardiogenic region of unlabelled hosts at HH5/6 and HH7/8. The embryos were allowed to develop over night as before. Terminal differentiation was assayed for using the MF20 antibody (Fig.4, red staining); GFP expression was enhanced using an anti-GFP antibody (Fig.4, green staining).

The location of GFP-positive cells was established by fluorescence microscopy (Fig.4A-J), co-expression of sarcomeric myosins and GFP was analysed by confocal microscopy (Fig.4i-iii insets). We observed that the retention rate of tissue grafted into the cardiogenic region at HH5/6 was varied and grafts often dispersed, possibly because of the morphogenetic movements that lengthen the head at this time ((Cui et al., 2009; Redkar et al., 2001); n-numbers in Supplementary spreadsheet SS2). However, of the grafts that had been retained, only HH5/6 PHM ever expressed sarcomeric myosins, and only when grafted into the HH5/6 heart field (Fig.4Ai-iii). Grafts from older stages, and grafts transplanted into older hosts were surrounded by sarcomeric myosin-positive myocardium but did not express sarcomeric myosins themselves (Fig.4B-J, i-iii).

3.4. Non-myocardial programmes stimulated by Bmp

Our findings suggest that the PHM has cardiac competence up to HH5/6, but cardiac competence fades from HH7/8 onwards. Given that the PHM remains Bmp-sensitive, we asked: which programmes does Bmp control after HH5/6 instead of the cardiac programme? To test this, we returned to the 6-hours treatment regime, assaying the embryos for the expression of the PHM marker *Cyp26C1* (Fig.5A-Diii;), markers associated with the onset of the head skeletal muscle programme (*Pitx2*, *Tbx1*, *Msc*; Fig.5E-Piii) and markers associated with head and trunk skeletal muscle differentiation (*Six1*, *Eya1*, *Dach1*, *Dach2*, *Ebf2*, *Myf5*; Fig.6; (Bothe and Dietrich, 2006; Bothe et al., 2011) reviewed in (Schubert et al., 2018)). We also analysed markers associated with the vascular endothelial and endocardial programme (*Flk1=Kdr=VegfR2*, *NfatC1*; (Nimmagadda et al., 2005; Wu et al., 2011) Supplementary Figure SF6.A-Hiii) and markers associated with the smooth muscle programme (*Acta2=Sma*, *Tcf21=Capsulin*; Supplementary Figure SF6.I-Piii; (von Scheven et al., 2006b; Waldo et al., 2005)).

3.4.1. Bmp effect on head skeletal muscle markers

Our analysis showed that *Cyp26C1* and *Tbx1* were downregulated by Bmp at HH5/6, 7/8 and 9/10, in line with the idea that Bmp can lateralise the PHM at these stages (Fig.5A-C and M-O, red arrowheads). Bmp also downregulated *Pitx2* at HH5/6 (Fig.5E, red arrowhead); yet thereafter *Pitx2* expression remained stable (Fig.5F-Hiii, blue arrowheads). Notably, Bmp began to activate *Msc* at HH7/8 (Fig.5J), one stage earlier than reported by Bothe (2011), possibly because of the slightly higher Bmp concentration used in the current study. The upregulation of *Msc* was more pronounced at HH9/10 and HH13/14 (Fig.5K-Lii). Yet in the trunk, Bmp did not upregulate *Msc*, indicating a very specific role of Bmp in the activation of the head skeletal muscle programme.

For the genes associated with skeletal muscle differentiation, we found that Bmp downregulated *Six1* at HH5/6 to HH9/10 (Fig.6A-C, red arrowheads); the effect was mild at HH9/10, and no effect

was observed later (Fig.6Dii, blue arrowheads). *Eya1* was initially also suppressed (Fig.6E,F; red arrowheads). However, at HH9/10 and 13/14, *Eya1* was upregulated (Fig.6G, Hii; green arrowhead). The expression of the *Dach* and *Ebf* genes was not affected except for some upregulation of *Dach2* in the neural plate (Fig.6M, green arrow). At HH13/14, *Myf5* expression was slightly downregulated in the pharyngeal muscle anlagen (Fig.6Uii, red arrowhead), but not in the anlage of the lateral rectus muscle (Fig.6Uii, blue arrowhead). In the trunk, *Six1* and *Myf5* were downregulated (Fig.6Diii, Uiii), *Dach1* and *Dach2* were downregulated close to the bead and upregulated at a distance where Bmp concentrations are lower (Fig.6Liii, Piii), *Eya1* was upregulated (Fig.6Hiii). Thus, both in the head and in the trunk, Bmp supports *Eya1* expression, but hinders genes readying cells for terminal skeletal muscle differentiation such as *Myf5*. Taken together, our data specifically on *Msc* and *Eya1* suggest that at the time that cardiac competence of the PHM fades, Bmp promotes the entry into the programme for head skeletal myogenesis.

3.4.2. Bmp effect on vascular endothelial, endocardial and smooth muscle markers

Bmp has been shown to stimulate *Kdr* expression and vascular endothelial cell formation in the somites, and our findings corroborate this notion ((Nimmagadda et al., 2005), SF6, Diii). In the head, however, Bmp between stages HH5/6 and HH9/10 rather reduced *Kdr* expression (SF6, A-C). This was unexpected and warrants further investigation. The expression of *NfatC1* was not changed in the mesoderm, but at HH13/14, expression was upregulated in the pharyngeal endoderm (SF6, Hii, green arrows). *Acta2* was upregulated at HH5/6 to HH9/10 (SF6, I-K, green arrowheads), suggesting a prolonged competence of the PHM to deliver smooth muscle. *Tcf21* however was only upregulated in the HH5/6 PHM (SF6, M-Piii; blue arrowheads).

3.5. Role of Wnt/beta Catenin signalling in the control of the cardiac versus the head skeletal muscle programme

Our study revealed that the PHM loses cardiac competence concomitant with the establishment of head skeletal muscle competence. Previous studies inferred that levels of Wnt/beta Catenin signalling might rise in the PHM at stages when we found its cardiac competence fades (Tzahor and Lassar, 2001). Thus, Wnt might promote the switch from cardiac to skeletal muscle competence observed here. On the other hand, Wnt/ beta Catenin signalling has been shown to suppress skeletal muscle formation in the head ((Tzahor et al., 2003) and Supplementary Fig. SF1). Wnt however has also been shown to contribute to the caudalisation of the embryo and hence may have more generic role in suppressing rostral programmes (Marvin et al., 2001). To investigate a possible role of Wnt/ beta Catenin signalling, we used the 6-hours experimental paradigm and performed three further tests: (1) We determined when exactly cardiogenesis is suppressed by Wnt3a, a ligand known to

trigger the beta-Catenin pathway ((Tzahor et al., 2003); Fig.7). (2) We tested whether at the early, cardiac-competent stages of the PHM, Bmp would induce *Szl=sFRP2-related*, a Wnt inhibitor strongly expressed in the early cardiac mesoderm and the SHF (Wittler et al., 2008), and whether at later stages, *Szl* would not be induced by Bmp any more (Fig.8A-Dii). As *Szl* is a marker for the cardiogenic mesoderm, we also tested the effect of Wnt3a for this marker (Fig.8E-Hii). (3) We tested whether Wnt3a would accelerate or repress the expression of markers for the PHM and head skeletal muscle precursors (Fig.9).

3.5.1. Effect of Wnt on cardiac markers

When Wnt3a-beads were inserted into the cardiogenic region of HH5/6 and HH7/8 embryos and the embryos left to develop for 6 hours, expression of *Nkx2*.5 was downregulated (Fig.7A,B; red arrowheads). However, when implanted at HH9/10, *Nkx2.5* expression was stable (Fig.7C, blue arrowheads). This suggests that cardiac cells are vulnerable to Wnt at early stages of their development. Focusing on stages HH7/8, then, we analysed the effect of Wnt on *Isl1* (Fig.7D), *Tbx2* (Fig.7E), *Hand2* (Fig.7F), *Gata4* (Fig.7G), *Tbx5* (Fig. 7H) and *Myocd* (Fig.7I). We found that Wnt mildly downregulated *Isl1*, and more strongly repressed *Tbx2*, *Tbx5* and *Myocd* (Fig.7D,E,H,I; red arrowheads), corroborating the early Wnt-sensitivity of cardiogenic cells. Yet the 6-hour Wnt exposure led to some upregulation of *Hand2* and *Gata4*, two of the markers more widely expressed in the lateral mesoderm, including in the trunk. This finding is consistent with a caudalising role of Wnt.

3.5.2. Effect of Bmp and Wnt on *Szl*

Testing the effect of Bmp and Wnt on the expression of the Wnt inhibitor *Szl*, we found that Bmp very strongly induced *Szl* at all stages examined (Fig.8A-Dii, green arrowheads). In contrast, Wnt did not affect *Szl* expression, neither in the early cardiogenic mesoderm (Fig.8E-G, blue arrowheads) nor in the HH13/14 pharyngeal arches (Fig.8Hi,ii; blue arrowheads). Thus, protection from Wnt signalling is available to cells responding to Bmp at all times. This suggest that the loss of cardiac competence in the PHM is not due to the elevation of Wnt signalling or loss of protection from Wnt.

3.5.3. Effect of Wnt on markers for the PHM and head skeletal muscle precursors

When Wnt3a-beads were implanted into the PHM, they downregulated the PHM marker *Cyp26C1* at HH5/6, HH7/8 and HH9/10, but not at HH13/14 (Fig.9A-Dii). This downregulation occurred already after 2 hours (Supplementary Fig. SF2,V), identifying *Cyp26C1* as the most Wnt-sensitive marker in our study. Wnt3a also downregulated *Pitx2* at HH5/6 and HH7/8 (Fig.9E,F; red arrowheads), and prevented the onset of *Msc* at HH9/10 (Fig.9K, ref arrowhead). Wnt at times mildly expanded the expression domains of *Tbx1* in a rostral direction (Fig.9A,B; green arrowheads) or upregulated rostral

Eya1 levels to those found more caudally (Fig.9W, green arrowheads), in line with a generic caudalising role of Wnt. Wnt3a however had no effect on *Six1* and *Myf5* expression in the head (Fig.9Q-Tii; Fig.9Yi-ii; blue arrowheads) whilst expression in the trunk was slightly upregulated (Fig.9Tiii, Yiii; green arrowheads). Taken together, within the six-hours time-frame used here, Wnt had a negative effect on PHM markers and the head skeletal muscle programme, likely targeting PHM/ head skeletal muscle precursor cells.

4. Discussion

Various forms of cell labelling/ cell tracing experiments have mapped the fate of the early gastrulating mes-endoderm, i.e. established the normal developmental programmes or trajectories of cells left undisturbed. These studies showed that cells gastrulating from the HH3 chicken primitive streak and settling in a position lateral to the boundary of the overlying neural plate will deliver the primitive heart that starts beating at HH10 ((Camp et al., 2012; Garcia-Martinez and Schoenwolf, 1993); reviewed in (Sendra et al., 2021; Wittig and Münsterberg, 2020)). In contrast, cells that settle in a paraxial position contribute to the skull and to craniofacial skeletal muscles (reviewed in (Schubert et al., 2018). The fate of the cells at the paraxial-lateral interface is somewhat unclear, likely because these cells are multipotent and able to contribute to the SHF/heart, to its smooth muscle collar, to the great vessels as well as head skeletal muscle.

Exposing the head mesoderm to molecular challenges has led to an enormous body of knowledge regarding the extrinsic factors (signalling molecules, but also tissue tension) and the intrinsic factors (downstream modulators of signals and transcription factors) that control normal development. However, the distinction between cell fate and the often much wider cellular competence or potency, i.e. the ability to engage in a programme, has rarely been addressed. In addition, the timescale of experiments has often led to differing views on the state of cellular commitment or plasticity, with cell specification, i.e. the reversible commitment of cells to a developmental programme, and cell determination, i.e. the irreversible commitment of cells to a developmental programme, not always being distinguished. Here in this study, we aimed to establish whether there is a generic cardiac competence in the head mesoderm, encompassing the paraxial head mesoderm (PHM) that is not fated to contribute to the heart.

4.1. At early headfold stages, the PHM is heart-competent

Using a strict 6-hour regime to treat the chicken PHM with the cardiac promoter Bmp2, we found that up to early head fold stages at HH5/6, the PHM was able to activate the palette of transcription factors that cooperatively drives cardiogenesis in vitro and in vivo. Moreover, when given time to complete differentiation, the early PHM was able to do so, both when exposed to ectopic Bmp or when grafted into the cardiogenic region of a HH5/6 host. Thus, the entire head mesoderm is initially heart-competent, and cardiac-competence is the default state of the tissue. Notably, at early head fold stages, the PHM already expresses *Cyp26C1* that protects the tissue from caudalising retinoic acid. Moreover, it just about switched on *Pitx2* and *Tbx1*, two genes later involved in the activation of the skeletal muscle programme (Bothe and Dietrich, 2006; Bothe et al., 2007). This suggest that at HH5/6, the PHM is specified but not yet determined to follow its own developmental programme.

4.2. The cardiac competence of the PHM fades at early neurula stages

Between HH7-HH10, the ability of Bmp to trigger the cardiac programme in the PHM declined as fewer and fewer of the cardiac genes were able to respond. Moreover, the PHM was unable to complete cardiac differentiation. Genes that remained activatable were known Bmp pathway genes and genes associated with general lateral identity both in the trunk and the head mesoderm, indicating that the PHM remained Bmp-sensitive. This suggest that the PHM sheds specifically cardiac competence at early neurula stages. Previous studies had suggested that cardiogenesis can be triggered in the PHM as late as HH13/14 (Tirosh-Finkel et al., 2006). However, these studies treated embryos at HH9/10, just allowing them to develop for a longer time. Moreover, a more limited set of marker genes was analysed, and these markers included general lateral mesoderm markers that can lead to misinterpretation. Yet these data and ours can be reconciled: we found that at HH9/10, Bmp can still trigger the expression of *Isl1*, *Nkx2.5* and *Tbx2*, genes that, rather than being heart-specific, are expressed in various types of precursor cells, both in the endoderm and the ectoderm. One of the mesodermal cell types is smooth muscle, and we fund that smooth muscle actin (*Acta2*) can be activated by Bmp as late as HH10. This suggest that smooth muscle competence is retained longer than cardiac competence, in line with the requirement of the head mesoderm to finalise the cardiac outflow tract by adding its smooth muscle collar (Wang et al., 2017). At HH13/14, whilst Bmp cannot trigger expression of cardiac genes in the PHM within the 6-hours timeframe, it can dorsally expand the expression domain of *Isl1*. This phenotype was also reported for the long-exposure experiments (Tirosh-Finkel et al., 2006). *Isl1* remains strongly expressed in multipotent cells in the secondary heart field. Moreover, Bmp plays a role in recruiting cells from the secondary

heart field into the heart and into differentiation. Taken together, this suggest that at this late stage ectopic Bmp may dorsolaterally expand the area in the subpharyngeal mesoderm from which secondary heart field cells are being recruited.

4.3. At early neurula stages, the developmental competence of the PHM shifts to the head skeletal muscle programme

As embryos progressed from HH5/6 to HH7/8 and HH9/10, the response of the PHM to Bmp changed markedly. Initially, Bmp suppressed a wide palette of PHM marker genes including *Cyp26C1*, genes associated with the head programme of skeletal muscle formation (*Pitx2* and *Tbx1*), and genes generally involved in myogenesis (*Six1* and *Eya1*; reviewed in (Schubert et al., 2018)). These genes became more and more resistant to Bmp, with *Eya1* being upregulated by Bmp at HH9/10. Moreover, from HH7/8 onwards, Bmp activated *Msc*, a further upstream regulator of head skeletal myogenesis. This suggests that at the time cardiac competence fades, skeletal muscle competence is established. This however did not lead to a premature entry into differentiation. Skeletal muscle differentiation in the head does not commence before HH13/14 (Meireles Nogueira et al., 2015), and both for head and trunk skeletal muscle differentiation, Bmp is a strong inhibitor ((Tzahor et al., 2003; von Scheven et al., 2006a); reviewed in (Schubert et al., 2018)). Moreover, Msc, whilst activating *Myf5* at later stages (Moncaut et al., 2012), mainly acts as a transcriptional repressor (Harris et al., 2015), suggesting a scenario whereby the head skeletal muscle precursor genes establish myogenic competence but keep differentiation at bay to allow the expansion of the precursor pool first.

4.4. The shift from cardiac to skeletal muscle competence is intrinsic to the PHM

Previous studies suggested that from HH7/8 onwards, the cardiac programme may be repressed in the PHM owing to rising levels of beta-Catenin-mediated Wnt signalling (Tzahor and Lassar, 2001). We thus expected that ectopic Wnt3a application would promote the expression of PHM genes. However, this was not the case: Wnt3a suppressed the expression of most PHM and skeletal muscle associated genes in the same fashion as it repressed cardiac genes. At the same time, expression of genes representing more caudal positional values was upregulated and rostrally expanded, suggesting that Wnt participates in caudalising the mesoderm both in the paraxial and the lateral region ((Bressan et al., 2013; Marvin et al., 2001); this study). Compared to the Bmp effects, the Wnt effects were more subtle, probably because Wnt inhibitors are expressed in Hensen's node (*Crescent, Sfrp1, Dkk1*), the early endoderm (*Crescent, Sfrp1*), the neural plate/ neural tube next to

the PHM (*Sfrp1, Sfrp2, Sfrp3, Dkk2*), the notochord (*Dkk1*) and the lateral and cardiogenic mesoderm (*Szl*; see http://geisha.arizona.edu/geisha/), all protecting rostral tissues from the caudalising influence of Wnts produced in the primitive streak. Notably, Bmp strongly upregulated Szl in the PHM at all stages investigated. This indicates that Wnt protection was always induced, and hence the loss of cardiac competence in the PHM was not due to the overriding effects of Wnt.

The Wnt-independent loss of cardiac competence in the PHM, whilst not excluding other extrinsic factors, nonetheless points to an intrinsic control mechanism. This will require further investigation, but several lines of evidence support this idea: Msc is expressed during formation of the atrioventricular conduction system (von Scheven et al., 2006b), where it physically interacts with Gata4 to repress Cx30.2 (Harris et al., 2015). Msc may well interact with Gata4 or other proteins earlier to repress the cardiac programme in the PHM. Alternatively, as Msc bind to E-boxes similar to those recognised by MyoD (MacQuarrie et al., 2013), and Msc and MyoD binding sites have been predicted for the promoters of several cardiac genes (P. Mendes Vieira and S. Dietrich, unpublished observations), it may repress target genes directly. In a similar vein, Six1 contributes to the upregulation of pharyngeal Fgf8 expression which in turn upregulates *Tbx1* and *Msc* in the mesoderm (Bothe et al., 2011; Guo et al., 2011). Yet it may well have additional roles when it begins to be expressed in the early PHM.

4.5. Outlook

During vertebrate evolution, aspects of the skeletal muscle programme were recruited into the head mesoderm twice: first the effector genes required for muscle striation were brought under the control of smooth/cardiac upstream regulators, thereby creating powerful, yet tireless cardiac muscle ((Brunet et al., 2016) reviewed (Poelmann and Gittenberger-de Groot, 2019; Simões-Costa et al., 2005). Thereafter the core skeletal muscle regulators were recruited, diverting a subset of the head mesoderm to a skeletal muscle programme that allows voluntary control over the cranial openings (reviewed in (Schubert et al., 2018)). As PHM cells are relinquishing cardiac competence, they are potentially in a fragile state as the possibility to engage in skeletal muscle formation becomes available, but genes that enforce myogenesis are not expressed for a prolonged period of time. Pathological heart failure also creates a fragile state in which skeletal muscle-associated genes are de-repressed, most prominently Six1 which upregulates miR-25 that downregulates Serca2a (Oh et al., 2019). This suggest that there is a cardiac-skeletal muscle antagonism that requires tight control. Unravelling this mechanism will shed light onto normal development and will give deeper insight into cardiac disease.

Acknowledgements

We thank Soraya Idris-Anderson and Ashley Haywood for their assistance to the project, the IBBS section Epigenetics and Development for comments, and Frank Schubert for critically reading the manuscript. The work was funded by an UoP grant, an Erasmus Scholarship to N. Murciano and a BSDB Gurdon studentship to P. Mendes Vieira.

References

Alvares, L. E., Lours, C., El-Hanfy, A. and Dietrich, S. (2008). Microsurgical manipulation of the Notochord. *Methods Mol. Biol.* **461**, 289–303.

Andree, B., Duprez, D., Vorbusch, B., Arnold, H. H. and Brand, T. (1998). BMP-2 induces ectopic expression of cardiac lineage markers and interferes with somite formation in chicken embryos. *Mech Dev* **70**, 119–131.

Berti, F., Nogueira, J. M., Wöhrle, S., Sobreira, D. R. R., Hawrot, K., Dietrich, S., Meireles Nogueira, J., Wohrle, S., Sobreira, D. R. R., Hawrot, K., et al. (2015). Time course and side-by-side analysis of mesodermal, pre-myogenic, myogenic and differentiated cell markers in the chicken model for skeletal muscle formation. *J Anat* **227**, 361–382.

Bothe, I. and Dietrich, S. (2006). The molecular setup of the avian head mesoderm and its implication for craniofacial myogenesis. *Dev Dyn* **235**, 2845–2860.

Bothe, I., Ahmed, M. U., Winterbottom, F. L., Von Scheven, G. and Dietrich, S. (2007). Extrinsic versus intrinsic cues in avian paraxial mesoderm patterning and differentiation. *Dev Dyn* **236**, 2397–2409.

Bothe, I., Tenin, G., Oseni, A. and Dietrich, S. (2011). Dynamic control of head mesoderm patterning. *Development* **138**, 2807–2821.

Bressan, M., Liu, G. and Mikawa, T. (2013). Early mesodermal cues assign avian cardiac pacemaker fate potential in a tertiary heart field. *Science* **340**, 744–748.

Brown, C. O., Chi, X., Garcia-Gras, E., Shirai, M., Feng, X. H. and Schwartz, R. J. (2004). The Cardiac Determination Factor, Nkx2-5, Is Activated by Mutual Cofactors GATA-4 and Smad1/4 via a Novel Upstream Enhancer. *J. Biol. Chem.* **279**, 10659–10669.

Brunet, T., Fischer, A. H. L., Steinmetz, P. R. H., Lauri, A., Bertucci, P. and Arendt, D. (2016). The evolutionary origin of bilaterian smooth and striated myocytes. *Elife* **5**,.

Camp, E., Dietrich, S., Münsterberg, A. and Munsterberg, A. (2012). Fate mapping identifies the origin of SHF/AHF progenitors in the chick primitive streak. *PLoS One* **7**, e51948.

Chapman, S. C., Collignon, J., Schoenwolf, G. C. and Lumsden, A. (2001). Improved method for chick whole-embryo culture using a filter paper carrier. *Dev Dyn* **220**, 284–289.

Chen, Y. H., Ishii, M., Sun, J., Sucov, H. M. and Maxson, R. E. (2007). Msx1 and Msx2 regulate survival of secondary heart field precursors and post-migratory proliferation of cardiac neural crest in the outflow tract. *Dev. Biol.* **308**, 421–437.

Cui, C., Cheuvront, T. J., Lansford, R. D., Moreno-Rodriguez, R. A., Schultheiss, T. M. and Rongish, B. J. (2009). Dynamic positional fate map of the primary heart-forming region. *Dev. Biol.* **332**, 212–222.

Cui, M., Wang, Z., Bassel-Duby, R. and Olson, E. N. (2018). Genetic and epigenetic regulation of cardiomyocytes in development, regeneration and disease. *Development* **145**,.

Evans, D. J. and Noden, D. M. (2006). Spatial relations between avian craniofacial neural crest and paraxial mesoderm cells. *Dev Dyn* **235**, 1310–1325.

Gao, R., Liang, X., Cheedipudi, S., Cordero, J., Jiang, X., Zhang, Q., Caputo, L., Gunther, S., Kuenne, C., Ren, Y., et al. (2019). Pioneering function of Isl1 in the epigenetic control of cardiomyocyte cell fate. *Cell Res* **29**, 486–501.

Garcia-Martinez, V. and Schoenwolf, G. C. (1993). Primitive-streak origin of the cardiovascular system in avian embryos. *Dev Biol* **159**, 706–719.

Gessert, S. and Kühl, M. (2010). The multiple phases and faces of wnt signaling during cardiac differentiation and development. *Circ. Res.* **107**, 186–199.

Guo, C., Sun, Y., Zhou, B., Adam, R. M., Li, X., Pu, W. T., Morrow, B. E. and Moon, A. (2011). A Tbx1-Six1/Eya1-Fgf8 genetic pathway controls mammalian cardiovascular and craniofacial morphogenesis. *J Clin Invest* **121**, 1585–1595.

Hamburger, V. and Hamilton, H. L. (1951). A series of normal stages in the development of the chick embryo. *J. Morph.* **88**, 49–92.

Hami, D., Grimes, A. C., Tsai, H. J. and Kirby, M. L. (2011). Zebrafish cardiac development requires a conserved secondary heart field. *Development* **138**, 2389–2398.

Harris, J. P., Bhakta, M., Bezprozvannaya, S., Wang, L., Lubczyk, C., Olson, E. N. and Munshi, N. V.

(2015). MyoR modulates cardiac conduction by repressing Gata4. *Mol. Cell. Biol.* **35**, 649–661.

Hinck, A. P., Mueller, T. D. and Springer, T. A. (2016). Structural Biology and Evolution of the TGF-beta Family. *Cold Spring Harb Perspect Biol* **8**,.

Houyel, L. and Meilhac, S. M. (2021). Heart Development and Congenital Structural Heart Defects. *https://doi.org/10.1146/annurev-genom-083118-015012* **22**, 257–284.

Huminiecki, L., Goldovsky, L., Freilich, S., Moustakas, A., Ouzounis, C. and Heldin, C. H. (2009). Emergence, development and diversification of the TGF-beta signalling pathway within the animal kingdom. *BMC Evol Biol* **9**, 28.

Hutson, M. R., Zeng, X. L., Kim, A. J., Antoon, E., Harward, S. and Kirby, M. L. (2010). Arterial pole progenitors interpret opposing FGF/BMP signals to proliferate or differentiate. *Development* **137**, 3001–3011.

Ieda, M., Fu, J. D., Delgado-Olguin, P., Vedantham, V., Hayashi, Y., Bruneau, B. G. and Srivastava, D. (2010). Direct reprogramming of fibroblasts into functional cardiomyocytes by defined factors. *Cell* **142**, 375–386.

Jandzik, D., Garnett, A. T., Square, T. A., Cattell, M. V, Yu, J. K. and Medeiros, D. M. (2015). Evolution of the new vertebrate head by co-option of an ancient chordate skeletal tissue. *Nature* **518**, 534–537.

Jia, G., Preussner, J., Chen, X., Guenther, S., Yuan, X., Yekelchyk, M., Kuenne, C., Looso, M., Zhou, Y., Teichmann, S., et al. (2018). Single cell RNA-seq and ATAC-seq analysis of cardiac progenitor cell transition states and lineage settlement. *Nat Commun* **9**, 4877.

Klumpe, H. E., Langley, M. A., Linton, J. M., Su, C. J., Antebi, Y. E. and Elowitz, M. B. (2022). The context-dependent, combinatorial logic of BMP signaling. *Cell Syst.* **13**, 388-407.e10.

Kraus, Y., Aman, A., Technau, U. and Genikhovich, G. (2016). Pre-bilaterian origin of the blastoporal axial organizer. *Nat. Commun.* **7**,.

Kuratani, S. (2005). Craniofacial development and the evolution of the vertebrates: the old problems on a new background. *Zool. Sci* **22**, 1–19.

Li, T. W.-H., Ting, J.-H. T., Yokoyama, N. N., Bernstein, A., van de Wetering, M. and Waterman, M. L. (2006). Wnt activation and alternative promoter repression of LEF1 in colon cancer. *Mol. Cell. Biol.* **26**, 5284–5299.

Liberatore, C. M., Searcy-Schrick, R. D., Vincent, E. B. and Yutzey, K. E. (2002). Nkx-2.5 gene induction in mice is mediated by a Smad consensus regulatory region. *Dev Biol* **244**, 243–256.

Lien, C. L., McAnally, J., Richardson, J. A. and Olson, E. N. (2002). Cardiac-specific activity of an Nkx2-5 enhancer requires an evolutionarily conserved Smad binding site. *Dev Biol* **244**, 257–266.

Lopez-Sanchez, C., Garcia-Masa, N., Gañan, C. M., Garcia-Martinez, V., Ganan, C. M. and Garcia-Martinez, V. (2009). Movement and commitment of primitive streak precardiac cells during cardiogenesis. *Int J Dev Biol* **53**, 1445–1455.

Luna-Zurita, L., Stirnimann, C. U., Glatt, S., Kaynak, B. L., Thomas, S., Baudin, F., Samee, M. A., He, D., Small, E. M., Mileikovsky, M., et al. (2016). Complex Interdependence Regulates Heterotypic Transcription Factor Distribution and Coordinates Cardiogenesis. *Cell* **164**, 999–1014.

MacQuarrie, K. L., Yao, Z., Fong, A. P. and Tapscott, S. J. (2013). Genome-wide binding of the basic helix-loop-helix myogenic inhibitor musculin has substantial overlap with MyoD: Implications for buffering activity. *Skelet. Muscle* **3**,.

Marvin, M. J., Di Rocco, G., Gardiner, A., Bush, S. M. and Lassar, A. B. (2001). Inhibition of Wnt activity induces heart formation from posterior mesoderm. *Genes Dev.* **15**, 316–327.

Meilhac, S. M. and Buckingham, M. E. (2018). The deployment of cell lineages that form the mammalian heart. *Nat Rev Cardiol* **15**, 705–724.

Meireles Nogueira, J., Hawrot, K., Sharpe, C., Noble, A., Wood, W. M., Jorge, E. C., Goldhamer, D. J., Kardon, G. and Dietrich, S. (2015). The emergence of Pax7-expressing muscle stem cells during vertebrate head muscle development. *Front Aging Neurosci* **7**, 62.

Moncaut, N., Cross, J. W., Siligan, C., Keith, A., Taylor, K., Rigby, P. W. and Carvajal, J. J. (2012). Musculin and TCF21 coordinate the maintenance of myogenic regulatory factor expression levels during mouse craniofacial development. *Development* **139**, 958–967.

Morton, S. U., Quiat, D., Seidman, J. G. and Seidman, C. E. (2022). Genomic frontiers in congenital heart disease. *Nat. Rev. Cardiol.* **19**, 26–42.

Nimmagadda, S., Loganathan, P. G., Huang, R., Scaal, M., Schmidt, C. and Christ, B. (2005). BMP4 and noggin control embryonic blood vessel formation by antagonistic regulation of VEGFR-2 (Quek1) expression. *Dev. Biol.* **280**, 100–110.

Oh, J. G., Jang, S. P., Yoo, J., Lee, M. A., Lee, S. H., Lim, T., Jeong, E., Kho, C., Kook, H., Hajjar, R. J., et al. (2019). Role of the PRC2-Six1-miR-25 signaling axis in heart failure. *J. Mol. Cell. Cardiol.* **129**, 58–68.

Paffett-Lugassy, N., Singh, R., Nevis, K. R., Guner-Ataman, B., O'Loughlin, E., Jahangiri, L., Harvey, R. P., Burns, C. G. and Burns, C. E. (2013). Heart field origin of great vessel precursors relies on nkx2.5-mediated vasculogenesis. *Nat Cell Biol* **15**, 1362–1369.

Poelmann, R. E. and Gittenberger-de Groot, A. C. (2019). Development and evolution of the metazoan heart. *Dev. Dyn.* **248**, 634–656.

Redkar, A., Montgomery, M. and Litvin, J. (2001). Fate map of early avian cardiac progenitor cells. *Development* **128**, 2269–2279.

Schlange, T., Andree, B., Arnold, H. H. and Brand, T. (2000). BMP2 is required for early heart development during a distinct time period. *Mech Dev* **91**, 259–270.

Schubert, F. R., Singh, A. J., Afoyalan, O., Kioussi, C. and Dietrich, S. (2018). To roll the eyes and snap a bite - function, development and evolution of craniofacial muscles. *Semin Cell Dev Biol* **91**,.

Schultheiss, T. M., Burch, J. B. and Lassar, A. B. (1997). A role for bone morphogenetic proteins in the induction of cardiac myogenesis. *Genes Dev* **11**, 451–462.

Scuderi, G. J. and Butcher, J. (2017). Naturally Engineered Maturation of Cardiomyocytes. *Front Cell Dev Biol* **5**, 50.

Sendra, M., Domínguez, J. N., Torres, M. and Ocaña, O. H. (2021). Dissecting the Complexity of Early Heart Progenitor Cells. *J. Cardiovasc. Dev. Dis.* **9**,.

Shirai, M., Imanaka-Yoshida, K., Schneider, M. D., Schwartz, R. J. and Morisaki, T. (2009). T-box 2, a mediator of Bmp-Smad signaling, induced hyaluronan synthase 2 and Tgfbeta2 expression and endocardial cushion formation. *Proc Natl Acad Sci U S A* **106**, 18604–18609.

Si, L., Shi, J., Gao, W., Zheng, M., Liu, L., Zhu, J. and Tian, J. (2014). Smad4 mediated BMP2 signal is essential for the regulation of GATA4 and Nkx2.5 by affecting the histone H3 acetylation in H9c2 cells. *Biochem Biophys Res Commun* **450**, 81–86.

Simões-Costa, M. S., Vasconcelos, M., Sampaio, A. C., Cravo, R. M., Linhares, V. L., Hochgreb, T., Yan, C. Y. I., Davidson, B. and Xavier-Neto, J. (2005). The evolutionary origin of cardiac chambers. *Dev. Biol.* **277**, 1–15.

Sirard, C., Sammy, K., Mirtsos, C., Tadich, P., Hoodless, P. A., Itié, A., Maxson, R., Wrana, J. L. and Mak, T. W. (2000). Targeted disruption in murine cells reveals variable requirement for Smad4 in transforming growth factor beta-related signaling. *J. Biol. Chem.* **275**, 2063–2070.

Song, J., McColl, J., Camp, E., Kennerley, N., Mok, G. F., McCormick, D., Grocott, T., Wheeler, G. N.

and Munsterberg, A. E. (2014). Smad1 transcription factor integrates BMP2 and Wnt3a signals in migrating cardiac progenitor cells. *Proc Natl Acad Sci U S A* **111**, 7337–7342.

Spater, D., Hansson, E. M., Zangi, L. and Chien, K. R. (2014). How to make a cardiomyocyte. *Development* **141**, 4418–4431.

Tirosh-Finkel, L., Elhanany, H., Rinon, A. and Tzahor, E. (2006). Mesoderm progenitor cells of common origin contribute to the head musculature and the cardiac outflow tract. *Development* **133**, 1943–1953.

Tirosh-Finkel, L., Zeisel, A., Brodt-Ivenshitz, M., Shamai, A., Yao, Z., Seger, R., Domany, E. and Tzahor, E. (2010). BMP-mediated inhibition of FGF signaling promotes cardiomyocyte differentiation of anterior heart field progenitors. *Development* **137**, 2989–3000.

Tzahor, E. and Lassar, A. B. (2001). Wnt signals from the neural tube block ectopic cardiogenesis. *Genes Dev* **15**, 255–260.

Tzahor, E., Kempf, H., Mootoosamy, R. C. C., Poon, A. C. C., Abzhanov, A., Tabin, C. J. J., Dietrich, S. and Lassar, A. B. B. (2003). Antagonists of Wnt and BMP signaling promote the formation of vertebrate head muscle. *Genes Dev* **17**, 3087–3099.

van Wijk, B., Moorman, A. F. and van den Hoff, M. J. (2007). Role of bone morphogenetic proteins in cardiac differentiation. *Cardiovasc Res* **74**, 244–255.

von Scheven, G., Alvares, L. E., Mootoosamy, R. C. and Dietrich, S. (2006a). Neural tube derived signals and Fgf8 act antagonistically to specify eye versus mandibular arch muscles. *Development* **133**, 2731–2745.

von Scheven, G., Bothe, I., Ahmed, M. U., Alvares, L. E. and Dietrich, S. (2006b). Protein and genomic organisation of vertebrate MyoR and Capsulin genes and their expression during avian development. *Gene Expr Patterns* **6**, 383–393.

Waldo, K. L., Hutson, M. R., Ward, C. C., Zdanowicz, M., Stadt, H. A., Kumiski, D., Abu-Issa, R. and Kirby, M. L. (2005). Secondary heart field contributes myocardium and smooth muscle to the arterial pole of the developing heart. *Dev Biol* **281**, 78–90.

Wang, X. Y., Li, Y., Ma, Z. L., Wang, L. J., Chuai, M., Munsterberg, A., Geng, J. G. and Yang, X. (2013). Retention of stem cell plasticity in avian primitive streak cells and the effects of local microenvironment. *Anat Rec* **296**, 533–543.

Wang, X., Chen, D., Chen, K., Jubran, A., Ramirez, A. and Astrof, S. (2017). Endothelium in the pharyngeal arches 3, 4 and 6 is derived from the second heart field. *Dev Biol* **421**, 108–117.

Wittig, J. G. and Münsterberg, A. (2020). The Chicken as a Model Organism to Study Heart Development. *Cold Spring Harb. Perspect. Biol.* **12**, 1–17.

Wittler, L., Saborowski, M. and Kessel, M. (2008). Expression of the chick Sizzled gene in progenitors of the cardiac outflow tract. *Gene Expr. Patterns* **8**, 471–476.

Wu, B., Wang, Y., Lui, W., Langworthy, M., Tompkins, K. L., Hatzopoulos, A. K., Baldwin, H. S. and Zhou, B. (2011). Nfatc1 coordinates valve endocardial cell lineage development required for heart valve formation. *Circ Res* **109**, 183–192.

Wu, Y., Liu, X., Zheng, H., Zhu, H., Mai, W., Huang, X. and Huang, Y. (2020). Multiple roles of sFRP2 in cardiac development and cardiovascular disease. *Int. J. Biol. Sci.* **16**, 730–738.

Yamada, M., Revelli, J. P., Eichele, G., Barron, M. and Schwartz, R. J. (2000). Expression of chick Tbx-2, Tbx-3, and Tbx-5 genes during early heart development: evidence for BMP2 induction of Tbx2. *Dev Biol* **228**, 95–105.

Yue, Q., Wagstaff, L., Yang, X., Weijer, C. and Münsterberg, A. (2008). Wnt3a-mediated chemorepulsion controls movement patterns of cardiac progenitors and requires RhoA function. *Development* **135**, 1029–1037.

Zhou, L., Liu, Y., Lu, L., Lu, X. and Dixon, R. A. (2012). Cardiac gene activation analysis in mammalian non-myoblasic cells by Nkx2-5, Tbx5, Gata4 and Myocd. *PLoS One* **7**, e48028.

Figure Legends

Figure 1. The paraxial head mesoderm (PHM) is Bmp- and Wnt-responsive throughout.

Beads loaded with Bmp2 (A,B,C,Dii,Diii) or Wnt3a (E,F,G,Hii,Hiii) were implanted into the PHM or trunk paraxial mesoderm (somites) of chicken embryos at HH5/6, HH7/8, HH9/10 and HH13/14 as indicated at the top of the panel. Embryos were re-incubated for 6 hours and then analysed for the expression of the direct Bmp target *Msx2* and the direct Wnt target *Lef1* as indicated on the left. Images Di-iii and Hi-iii, respectively, are from the same embryo with Di, Hi showing the untreated control side. The position of the beads is marked by an asterisk, upregulated marker gene expression by a green arrowhead.

Bmp2-loaded beads strongly activated *Msx2* at all stages. Wnt3a-beads produced more subtle responses, but upregulated *Lef1*. Note that at stages HH5/6, HH7/8, HH9/10, the upregulated *Lef1* expression is a rostral extension of the normal expression domain, indicating that Wnt3a caudalised the tissue.

Abbreviations: ht, heart; hy, hyoid (2nd pharyngeal) arch; ma, mandibular (1st pharyngeal) arch; nt, neural tube; ov; otic vesicle; som, somite.

Figure 2. Bmp activates the full set of cardiac markers at HH5/6 only.

Beads loaded with Bmp2 were implanted into the PHM or somites of embryos at HH5/6, HH7/8, HH9/10 and HH13/14 as shown in Fig.1. After 6 hours of re-incubation, the embryos were assayed for cardiac and lateral mesoderm marker genes indicated on the left. These genes cooperatively drive cardiogenesis. Upregulated gene expression around the bead is indicated by green arrowheads, expanded expression domains by green arrows, unchanged expression by blue arrowheads. Note the declining responses to BMP after HH5/6.

Abbreviations: ect, surface ectoderm; end, endoderm; g, geniculate ganglion; ht, heart; hy, hyoid (2nd pharyngeal) arch; lm, lateral mesoderm; ma, mandibular (1st pharyngeal) arch; nt, neural tube; ov; otic vesicle; phm, paraxial head mesoderm; som, somite; Vo, ophthalmic division of the trigeminal (5th cranial) ganglion; Vmm maxillomandibular division of the (5th cranial) trigeminal ganglion, VII, facial (7th cranial) ganglion.

Figure 3. Longer exposure to Bmp allows the HH5/6 PHM to complete myocardial differentiation.

Implantation of control beads and beads loaded with 6.41µM or 19.23µM Bmp2 into the HH5/6, HH7/8, HH9/10 and HH13/14 PHM, followed by MF20-immunofluorescene to detect sarcomeric myosins (red staining). Embryos were left to develop for 6 hours (A-F) or overnight (G-R). (A,C,E,G,I,K,M,O,Q) show DIC images, (B,D,F,H,J,L,N,P,R) show the same embryo with fluorescence microscopy, respectively. Ectopic cardiomyocyte differentiation occurred around the bead after overnight incubation with 19.23µM Bmp2, but only in HH5/6 hosts (L, green arrowhead).

Figure 4. The HH5/6 PHM grafted into the HH5/6 cardiogenic environment can complete myocardial differentiation in vivo.

Tissue from GFP-expressing donors was implanted into unlabelled hosts as indicated for each image set. After overnight re-incubation, immunofluorescence to detect sarcomeric myosins (red) and enhance the GFP-signal (green) was performed. (A,B,C,D,E,F,G,H,I,J) are images of the heart obtained by compound fluorescence microscopy, ventral views; (i, ii, iii) are the corresponding confocal sections showing the red channel (i), the green channel (ii) and the overlay (iii). (I-Iiii) is the positive control, (J-Jiii) is the negative control. Note that the PHM derived from a HH5/6 donor differentiated when grafted into the cardiogenic environment of a HH5/6 host (A-Aiii). The PHM from older stages of development became incorporated into the host heart but did not differentiate.

Abbreviations: CM, cardiac mesoderm; PHM, paraxial head mesoderm; sp, segmental plate (pre-somitic mesoderm).

Figure 5. Changing responses to Bmp for the upstream regulators of the head skeletal muscle programme.

Implantation of Bmp2-beads and abbreviations as in Fig.1, 2. After 6h, the embryos were assayed for the expression of the early PHM marker *Cyp26C1* (A-Diii) and the three upstream regulators of head skeletal myogenesis, *Pitx2* (E-Hiii), *Msc* (I-Liii) and *Tbx1* (M-Piii). Upregulated gene expression around the bead is indicated by green arrowheads, downregulated expression by red arrowheads, unchanged expression by blue arrowheads; abbreviations s before. Note that after HH5/6, the negative influence of Bmp2 on these markers fades. *Pitx2* becomes refractory at HH7/8 (F) and *Msc* is upregulated (J).

Figure 6. Changing responses to Bmp for generic regulators of skeletal muscle formation.

Implantation of Bmp2-beads and annotations and abbreviations as in Fig.1, 2, 5; the green arrow points at upregulated expression in non-mesodermal tissues.

Note that initially, Bmp suppressed *Six1* and *Eya2* in the PHM, but this effect faded over time and at HH9/10 and HH13/14, Bmp upregulated *Eya1*, both in the head and in the trunk (G, Hii, Hiii). In the trunk, the Bmp concentration used here downregulated *Dach1* and *Dach2* expression close-by, but upregulated it at a distance; *Six1* and *Myf5* were always downregulated. In the head, *Myf5* was

slightly downregulated in the pharyngeal arch muscle anlagen and unaffected in the anlage of the lateral rectus eye muscle (Ui, Uii; lr).

Figure 7. Wnt3a suppresses some cardiac markers as HH5/6 and HH7/8.

Ventral views of embryos with Wnt3a-loaded beads implanted into the lateral/cardiogenic mesoderm at HH5/6 (A), HH7/8 (B, D-I) and HH9/10 (C). After 6 hours of re-incubation, embryos were assayed for the markers indicated on top of each image. Note that *Nkx2.5*, *Isl1*, *Tbx2*, *Tbx5*, *Myocd* were downregulated (A,B,D,E,H,I; green arrowheads); *Hand2* and *Gata4*, two genes also expressed in the trunk lateral mesoderm were upregulated (red arrowheads). At HH9/10, markers were refractory (shown for *Nkx2.5*; C, blue arrowhead).

Figure 8. Effect of Bmp and Wnt on the Wnt-inhibitor *Szl*.

(A-Dii) Bmp2-loaded beads were implanted into the PHM of HH5/6, HH7/8, HH9/10 and HH13/14 embryos as in Fig.1; embryos were re-incubated for 6 hours. Dorsal views in (A-C), lateral views in (Di,Dii). *Szl* was strongly upregulated at all times.

(E-Hii) Wnt3-loaded beads were implanted into the lateral/ cardiogenic mesoderm of HH5/6, HH7/8, HH9/10 embryos as shown in Fig.7, and into the pharyngeal mesoderm of HH13/14 embryos as in (Dii). Ventral views in (E-G), lateral views in (Hi,Hii). Wnt3a did not affect *Szl* expression.

Abbreviations as in Fig.1 for all.

Figure 9. Effect of Wnt3a on markers for the PHM, the head programme of myogenesis and generic skeletal muscle markers.

Wnt3a-loaded beads were implanted into the PHM of HH5/6, HH7/8, HH9/10 and HH13/14 embryos as in Fig.1E-Hiii and Fig.7E-Hii. After 6 hours, embryos were assayed for the expression of marker genes shown on the left of the panel; annotations and abbreviations as before. In the head, Wnt3a suppressed the expression of *Cyp26C1*, *Pitx2* and *Msc* (A-C, E-F, K; red arrowheads), slightly expanded the expression domain of *Tbx1* (M,N; green arrowheads) and slightly elevated *Eya1* expression to levels found in the trunk (V, green arrowhead). At stages HH13/14, these markers were unaffected (Dii-Pii; blue arrowheads) as was *Myf5* (Xii; blue arrowhead). In the trunk, Wnt3a elevated the expression of *Six1* and *Myf5* (Tiii, Xiii).

Figure 10. Graphical Summary.

The head mesoderm has full cardiac competence until HH5/6, and prolonged smooth muscle competence until HH9/10. In the PHM, the head skeletal muscle programme becomes available as cardiac competence declines.

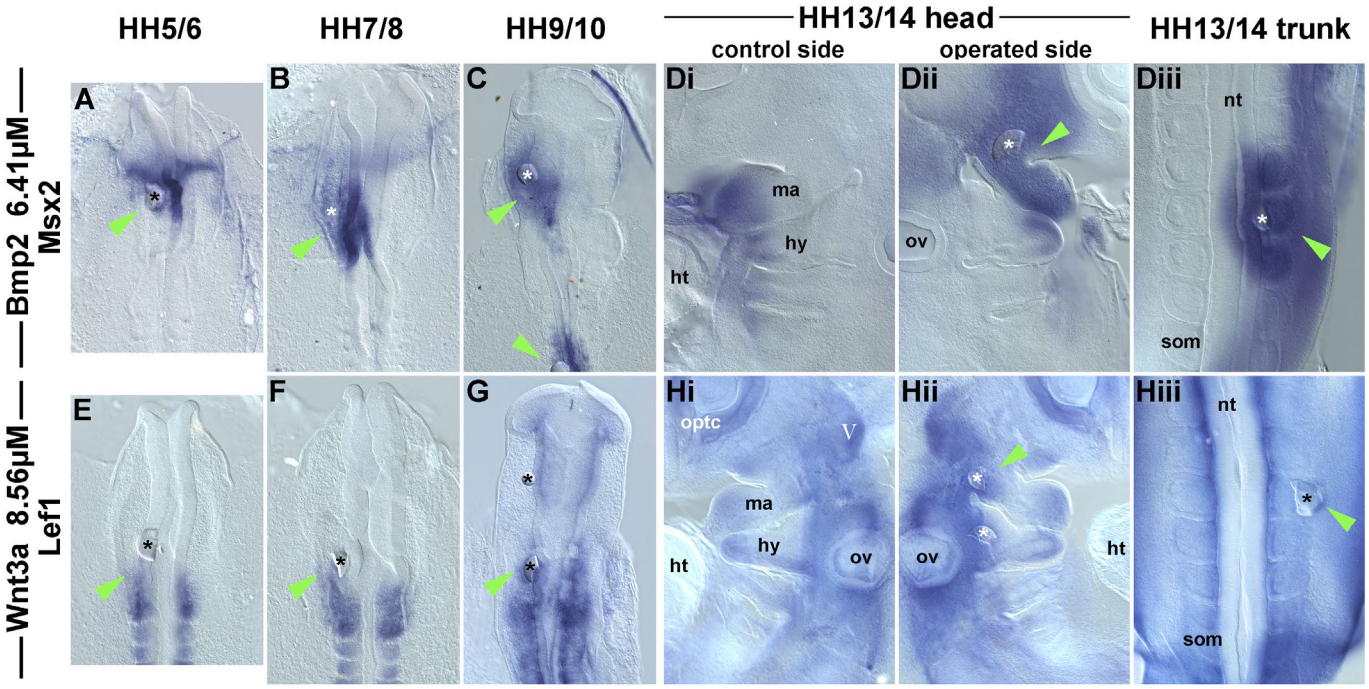
HH5/6
HH7/8
HH9/10
HH13/14 head
control side
operated side
HH13/14 trunk
Bmp2 6.41μM
Msx2
Wnt3a 8.56μM
Lef1
A
B
C
Di
Dii
Diii
E
F
G
Hi
Hii
Hiii
ma
hy
ht
ov
nt
som
optc
V

Fig.1

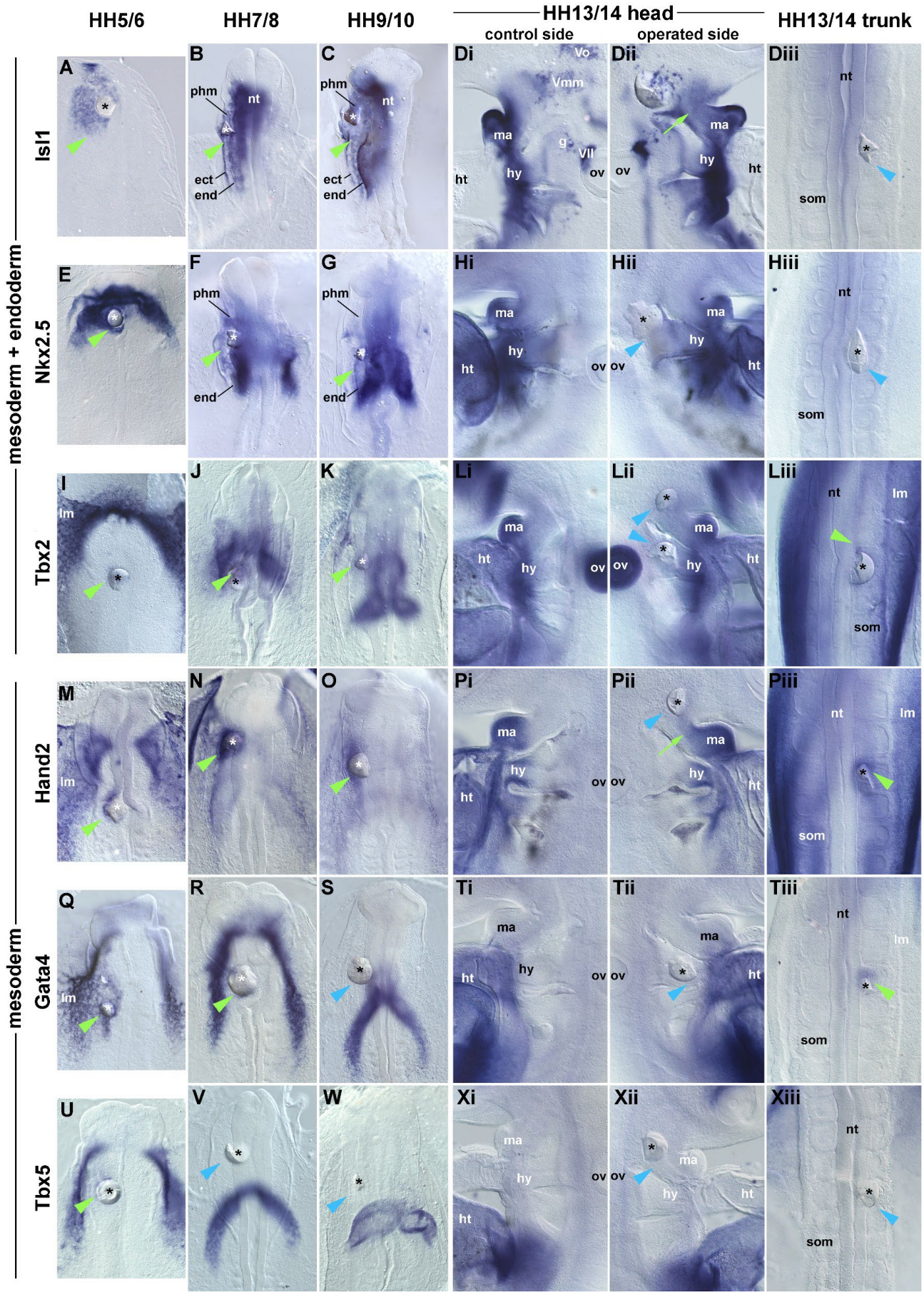
HH5/6
HH7/8
HH9/10
HH13/14 head
control side
operated side
HH13/14 trunk
mesoderm + endoderm
mesoderm
Isl1
Nkx2.5
Tbx2
Hand2
Gata4
Tbx5
A
B
C
Di
Dii
Diii
E
F
G
Hi
Hii
Hiii
I
J
K
Li
Lii
Liii
M
N
O
Pi
Pii
Piii
Q
R
S
Ti
Tii
Tiii
U
V
W
Xi
Xii
Xiii
phm
nt
ect
end
Vo
Vmm
ma
g
VII
hy
ov
ht
lm
som

Fig.2

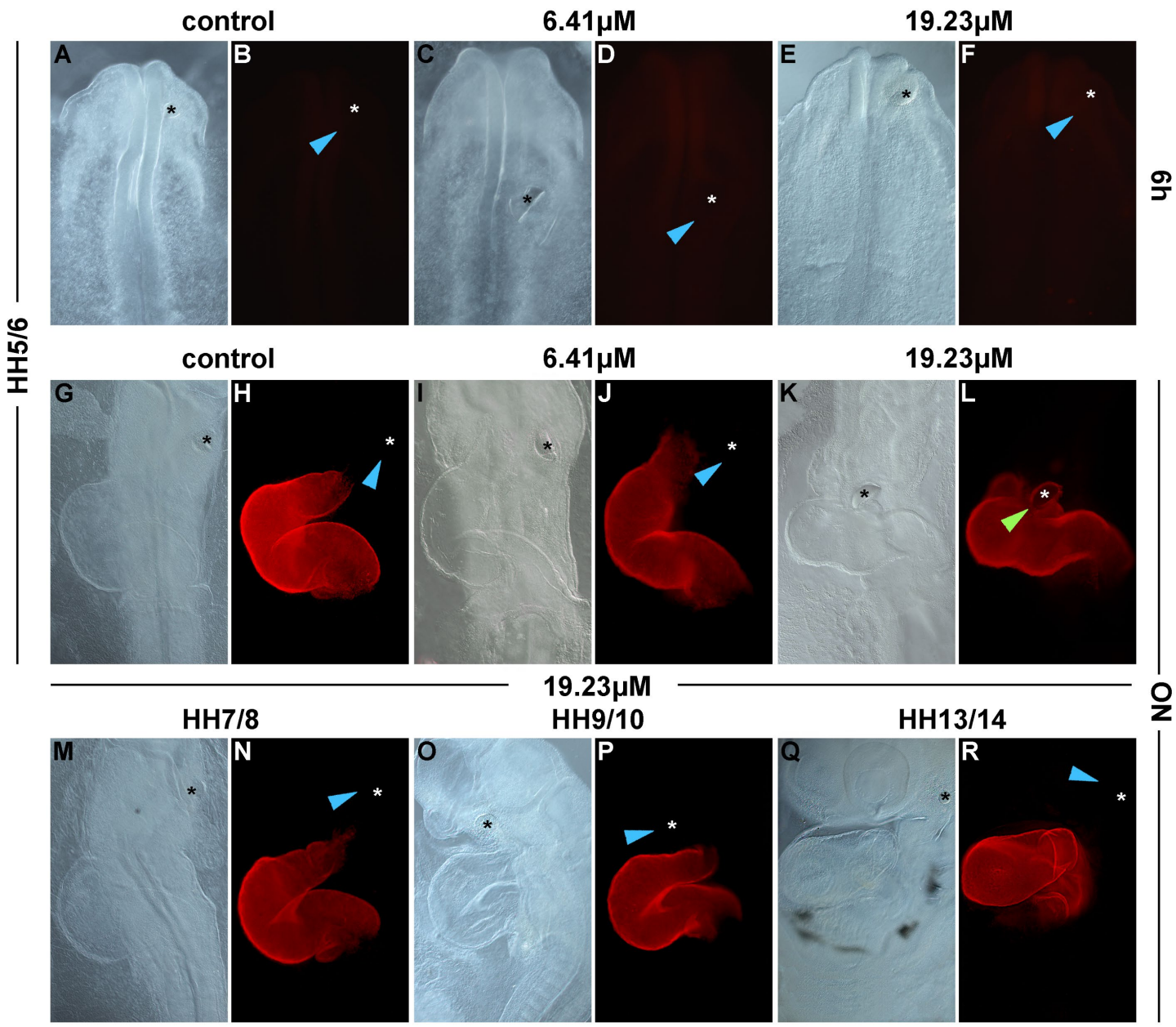
control
6.41μM
19.23μM
A
B
C
D
E
F
6h
HH5/6
control
6.41μM
19.23μM
G
H
I
J
K
L
19.23μM
ON
HH7/8
HH9/10
HH13/14
M
N
O
P
Q
R

Fig.3

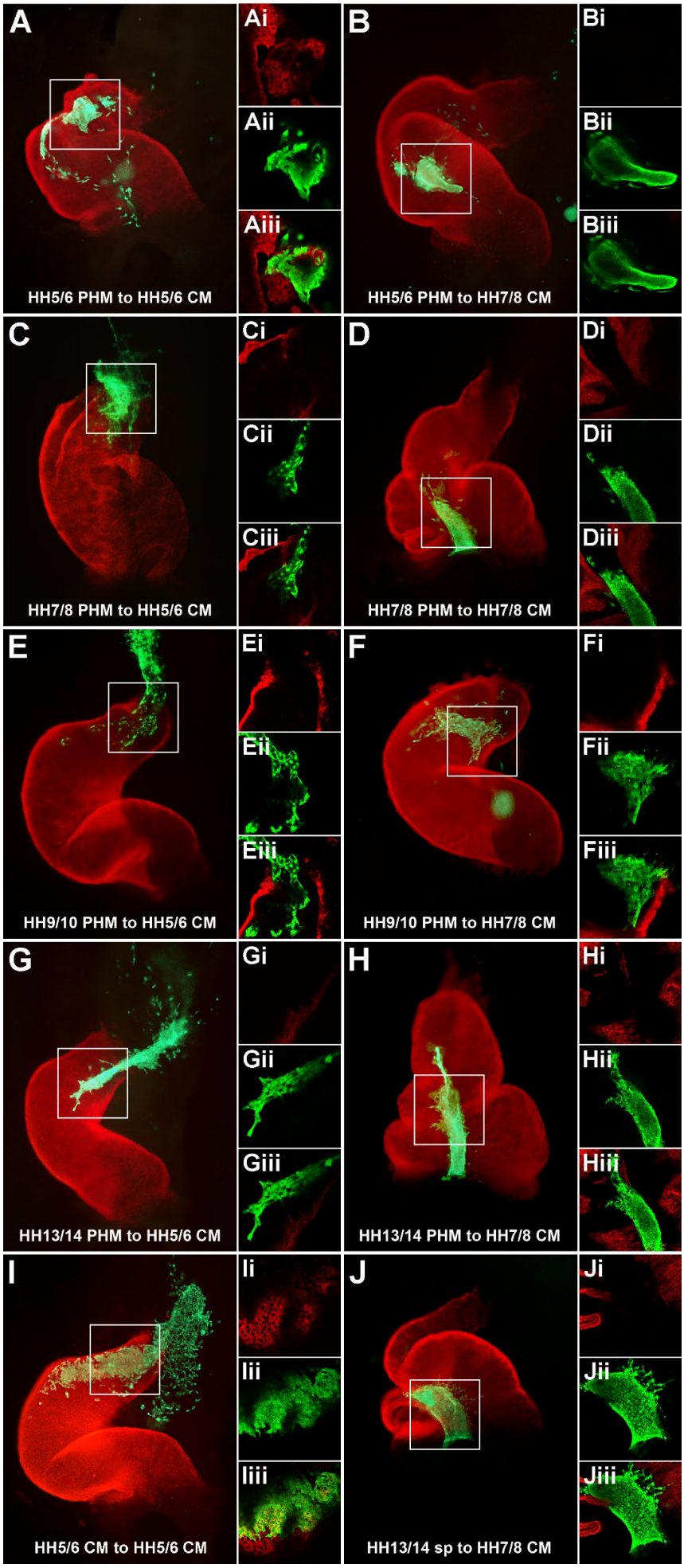
A
Ai
Aii
Aiii
HH5/6 PHM to HH5/6 CM
B
Bi
Bii
Biii
HH5/6 PHM to HH7/8 CM
C
Ci
Cii
Ciii
HH7/8 PHM to HH5/6 CM
D
Di
Dii
Diii
HH7/8 PHM to HH7/8 CM
E
Ei
Eii
Eiii
HH9/10 PHM to HH5/6 CM
F
Fi
Fii
Fiii
HH9/10 PHM to HH7/8 CM
G
Gi
Gii
Giii
HH13/14 PHM to HH5/6 CM
H
Hi
Hii
Hiii
HH13/14 PHM to HH7/8 CM
I
Ii
Iii
Iiii
HH5/6 CM to HH5/6 CM
J
Ji
Jii
Jiii
HH13/14 sp to HH7/8 CM

Fig.4

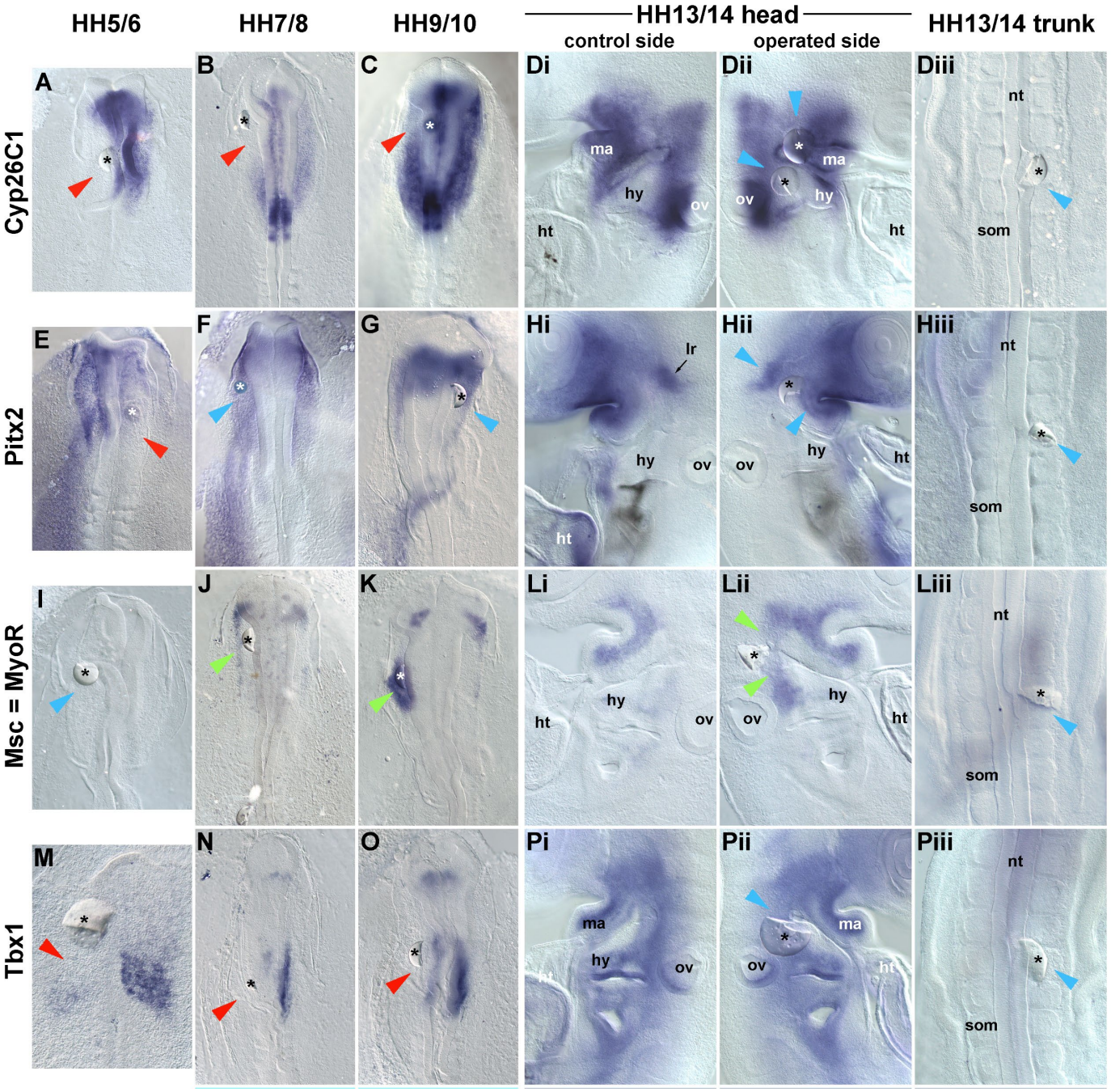
HH5/6
HH7/8
HH9/10
HH13/14 head
control side
operated side
HH13/14 trunk
Cyp26C1
Pitx2
Msc = MyoR
Tbx1
A
B
C
Di
Dii
Diii
E
F
G
Hi
Hii
Hiii
I
J
K
Li
Lii
Liii
M
N
O
Pi
Pii
Piii
ma
hy
ov
ht
lr
nt
som

Fig.5

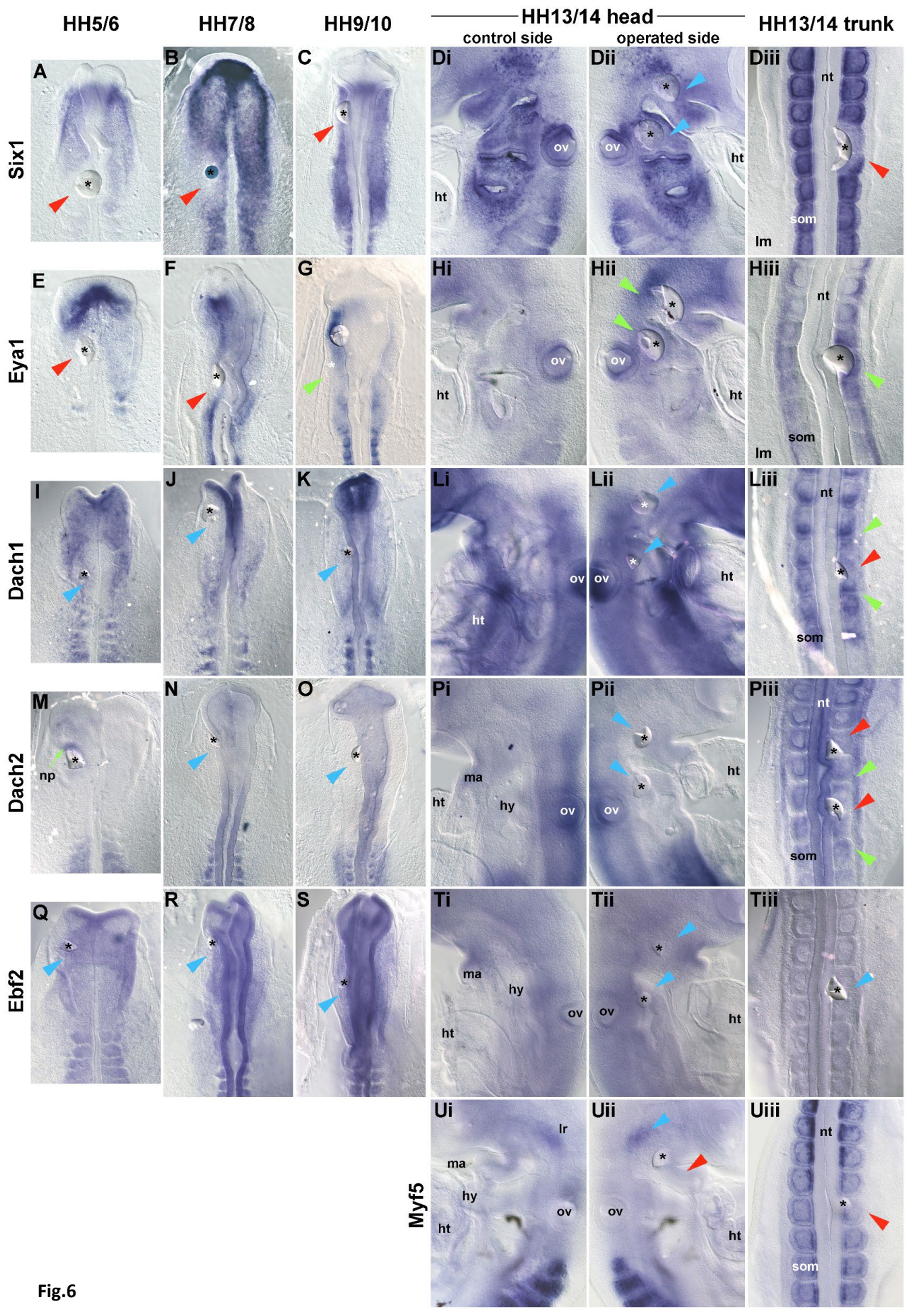
HH5/6
HH7/8
HH9/10
HH13/14 head
control side
operated side
HH13/14 trunk
Six1
Eya1
Dach1
Dach2
Ebf2
Myf5
A
B
C
Di
Dii
Diii
E
F
G
Hi
Hii
Hiii
I
J
K
Li
Lii
Liii
M
N
O
Pi
Pii
Piii
Q
R
S
Ti
Tii
Tiii
Ui
Uii
Uiii
ov
ht
nt
som
lm
np
ma
hy
lr

Fig.6

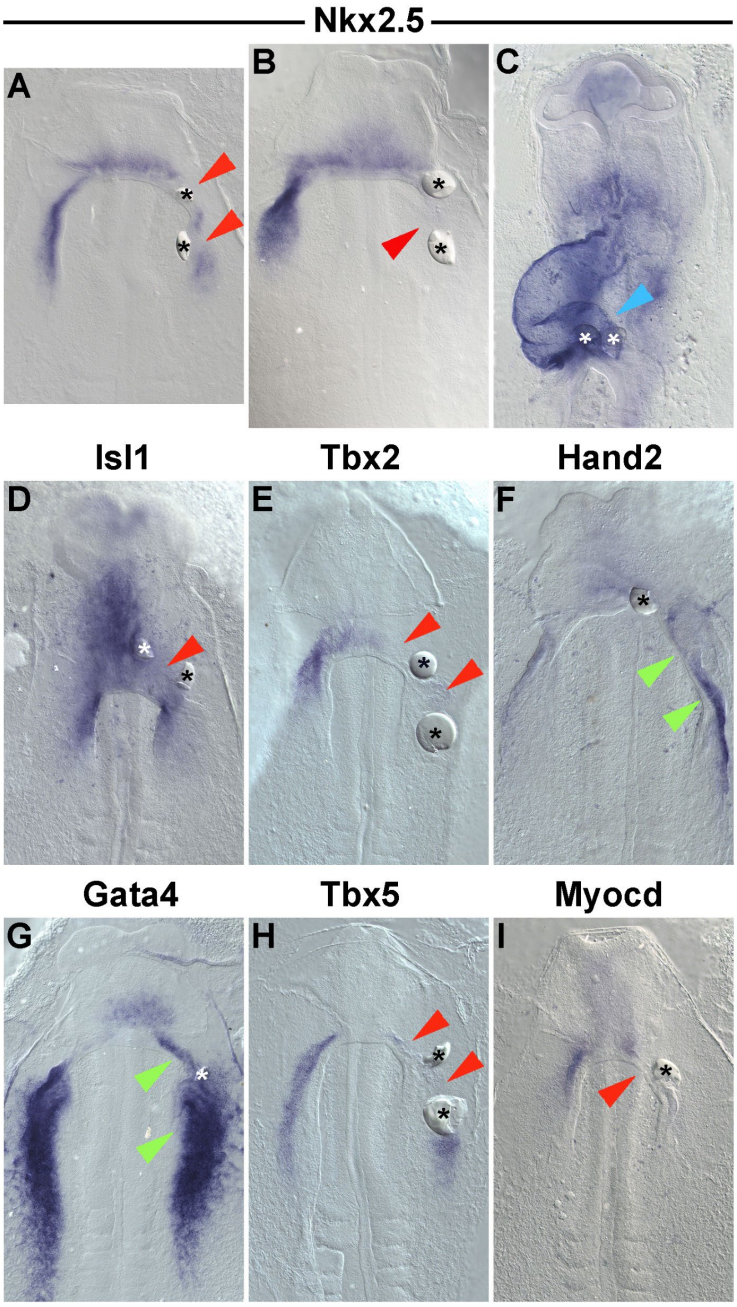

Fig.7

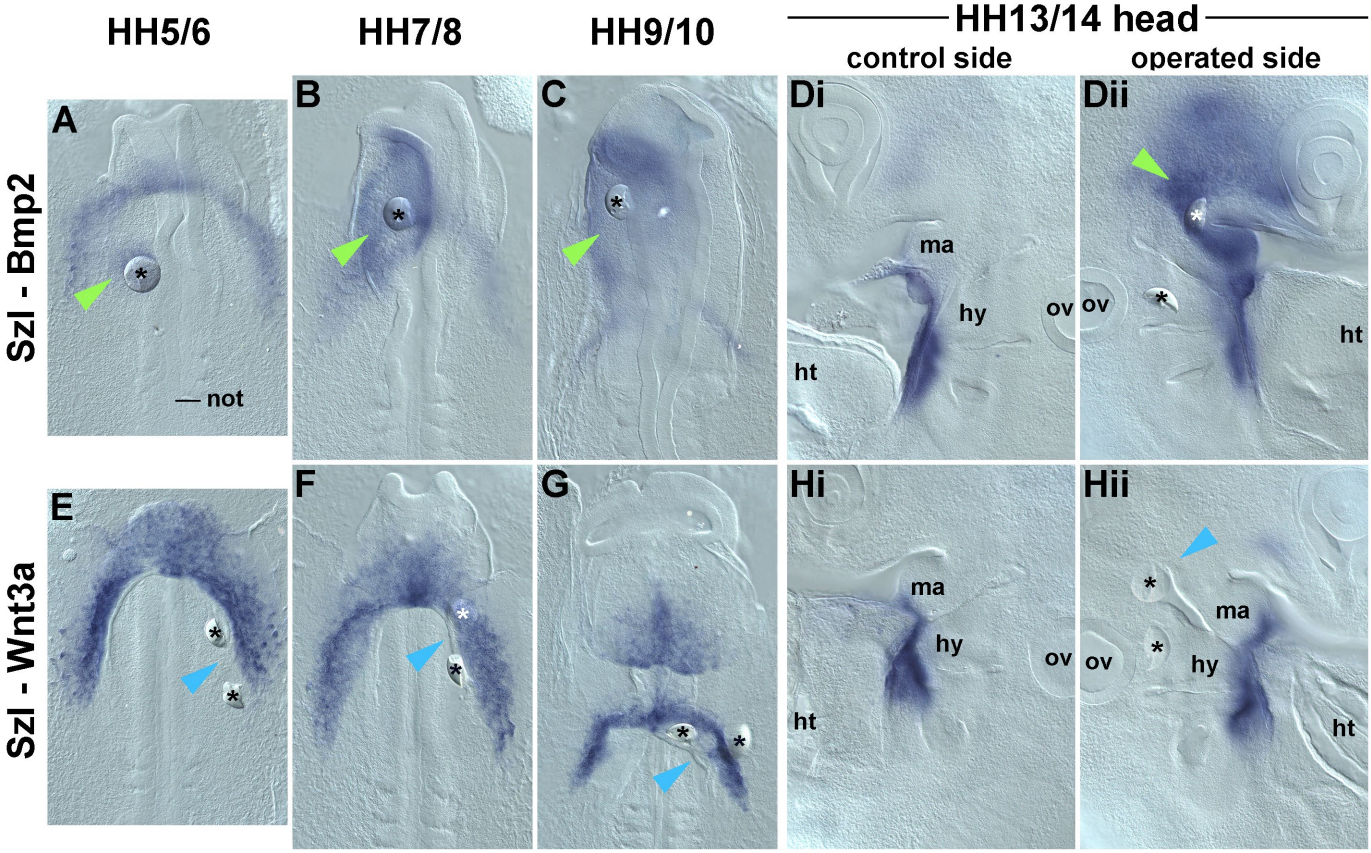
HH5/6
HH7/8
HH9/10
HH13/14 head
control side
operated side
Szl - Bmp2
Szl - Wnt3a
A
B
C
Di
Dii
E
F
G
Hi
Hii
not
ma
hy
ov
ht

Fig.8

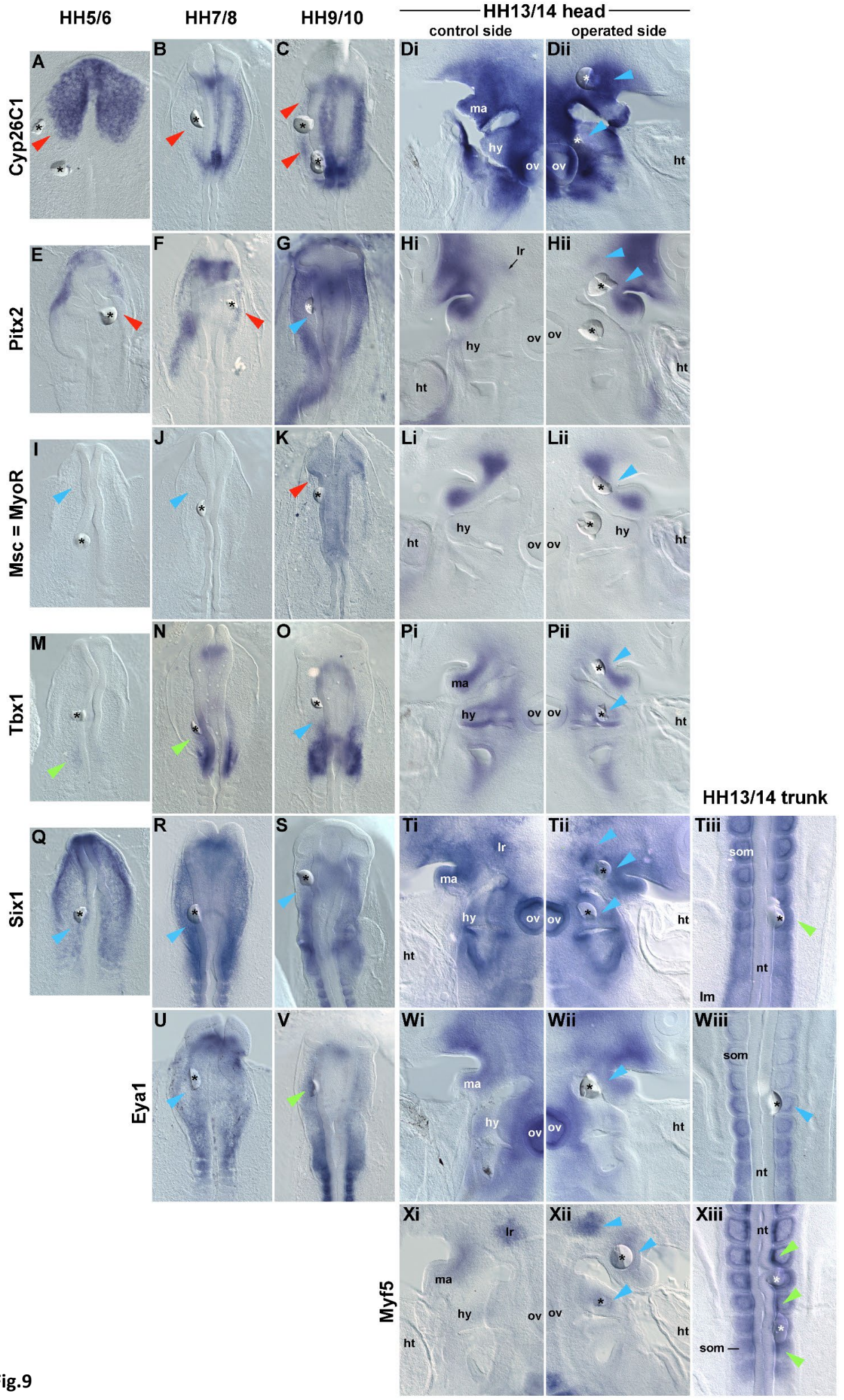
HH5/6
HH7/8
HH9/10
HH13/14 head
control side
operated side
HH13/14 trunk
Cyp26C1
Pitx2
Msc = MyoR
Tbx1
Six1
Eya1
Myf5
A
B
C
Di
Dii
E
F
G
Hi
Hii
I
J
K
Li
Lii
M
N
O
Pi
Pii
Q
R
S
Ti
Tii
Tiii
U
V
Wi
Wii
Wiii
Xi
Xii
Xiii
ma
hy
ov
ht
lr
som
nt
lm

Fig.9

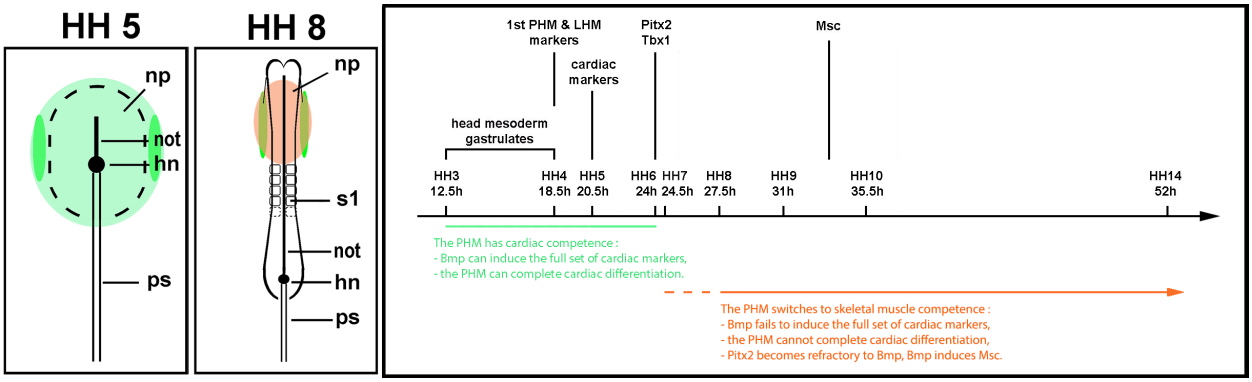
HH 5
np
not
hn
ps
HH 8
np
s1
not
hn
ps
1st PHM & LHM markers
Pitx2
Tbx1
Msc
cardiac markers
head mesoderm gastrulates
HH3 12.5h
HH4 18.5h
HH5 20.5h
HH6 24h
HH7 24.5h
HH8 27.5h
HH9 31h
HH10 35.5h
HH14 52h
The PHM has cardiac competence :
- Bmp can induce the full set of cardiac markers,
- the PHM can complete cardiac differentiation.
The PHM switches to skeletal muscle competence :
- Bmp fails to induce the full set of cardiac markers,
- the PHM cannot complete cardiac differentiation,
- Pitx2 becomes refractory to Bmp, Bmp induces Msc.

Fig.10